[UCI]I804:21031-000002238299

Thesis for the Degree of Doctor of Philosophy

A Study on Dynamics of Network Properties in Scientific Phenomena

by

Seungsik Min
Department of Physics
The Graduate School
Pukyong National University

February 2016

A Study on Dynamics of Network Properties in Scientific Phenomena

과학적 현상에서 네트워크 성질의 동역학 연구

Advisor: Prof. Kyungsik Kim

by
Seungsik Min

A thesis submitted in partial fulfillment of the requirements
for the degree of

Doctor of Philosophy

in Department of Physics, Graduate School,
Pukyung National University

February 2016

민승식의 이학박사 학위 논문을 인준함.

2016년 2월

심사위원장	이학박사	이 영 섭	(인)
심사위원	공학박사	하 덕 호	(인)
심사위원	이학박사	정 재 원	(인)
심사위원	이학박사	임 규 창	(인)
심사위원	이학박사	김 경 식	(인)

A Study on Dynamics of Network Properties in Scientific Phenomena

Seungsik Min

Department of Physics, Graduate School,
Pukyung National University

ABSTRACT

In recent years, research on complex systems are actively conducted across several disciplines including physics, biology, earth science, economy, and social science, etc. A complex system is made up of numerous components with complex interactions among them, which results in a macroscopic phenomenon of the whole system more than the sum of the parts. In order to understand the complex system as holistic perspectives, researchers usually take a network or graph theory. The network is a set constituted of nodes and their links, and use the adjacency matrix to descript the links of nodes.

Network theory in discrete mathematics has acted as a wonderful language to express a complex system since the 1960s. Starting from the study of random network by Erdös and Rény (ER) in 1961, Watts and Strogatz (WS) clarified the actor network, C. elegans network, and electrical power network have small-worldness using clustering coefficient in 1998. Also, Barabási and Albert (BA) investigated the scale-free properties of complex networks in 1999. Thereafter, researches on complex networks have evolved explosively by a variety of methods and data.

In this paper, we construct several networks in biology, earth science, economics, and social science in various methods. Analyzing the network properties in multiple ways, we derived the dynamics of network properties.

First, we investigate the interacting amino acids in protein structures as an example of biological system. It is shown from our result that protein networks have a small-world feature regardless of their structural class (α, β, $\alpha+\beta$, and α/β). Also, proteins are particularly found to have the positive assortative coefficient that applied to the topological property described as a tendency of connectivity of high-degree nodes. The modularity of the proteins in our case is significantly large as an increasing function of the number of amino acids in each protein.

Second, we study the seismic network of California in USA as an example of geological system. We performed the computer simulation from seismic time series data taken in southern California. After simulating a seismic network against spatial shifts and scales in a volume, we treat the feature of the topological properties more briefly via various statistical quantities such as the probability distribution of degree, characteristic path length, mean clustering coefficient, small-worldness, cost efficiency, global efficiency, modularity, and assortative coefficient.

Third, we study the seismic network more profound using Japan earthquake time series. Seismic network is investigated by considering the volume resolution and the temporal causality. A computer simulation of seismic networks is performed from seismic time series data taken in Japan. For our case, the universal and irregular properties of statistical quantities in seismic network do not find unambiguously, but it may be inferred that these topological properties improve by implementing the method and its technique from registered data of seismic networks.

Forth, we investigate the visibility network in a time series of the KOSPI and the KOSDAQ indices converting by the visibility algorithm. As a data, we extract the indices from the KOSPI and KOSDAQ that are exchanged on the Korean stock market during a period 1996–2014. The KOSPI and the KOSDAQ by adopting the visibility algorithm is proportional to a power law rather than the Poisson distribution. We mainly simulate and analyze the network metrics from the nodes and its links in the financial networks. The universal and irregular properties of statistical quantities in financial network do not find unambiguously, but it may be inferred that these topological properties improve by implementing the statistical method and its technique from registered data of financial networks.

Lastly, we study the microscopic community structure of the Korean meteorological society in the author network. Through oscillator networks, we simulate and analyze the averaged communicability functions such as the G_p^{EA}, G_p^{RA}, G_p^{EL}, and $1/G_p^{D}$. After constructing networks triggered an equally contributed weight between the first author and other authors in one published paper, we mainly treat these structures of communicability from these averaged communicability functions. The function E_p^{EL} has a commutative relation stronger than the other three, and our results support the development of the adaptability and the stability of social organization for an individual.

Keywords: Protein, Amino acid, Biological network, Seismic network, Visibility graph, KOSPI, KOSDAQ, Communicability function, Oscillator network, Community structure, Complex network, Small-worldness, Scale-free network, Dynamics of network property, Degree distribution, Characteristic path length, Clustering coefficient, Efficiency, Assortative coefficient, Modularity

CONTENTS

Abstract i
Contents iv
List of Figures and Tables v

Ⅰ. Introduction **1**

1. BIOLOGICAL SYSTEM: Protein Contact Network of Amino Acid 1
2. GEOLOGICAL SYSTEM: Seismic Network of California in USA 3
3. GEOLOGICAL SYSTEM: Seismic Network of Japan 5
4. ECONOMIC SYSTEM: Visibility Network of Korea Stock Market 7
5. SOCIAL SYSTEM: Communicability Network for Authors of Korean Meteorological Society 9

Ⅱ. Methodology **10**

1. General Network Properties 10
2. Protein Contact network in Biological system 13
3. Seismic Network in Geological System 14
4. Visibility Network in Economic System 14
5. Network communicability in Social System 15

Ⅲ. Results of Network Properties in Scientific Phenomena **21**

1. BIOLOGICAL SYSTEM: Protein Contact Network of Amino Acid 21
2. GEOLOGICAL SYSTEM: Seismic Network of California in USA 27
3. GEOLOGICAL SYSTEM: Seismic Network of Japan 33
4. ECONOMIC SYSTEM: Visibility Network of Korea Stock Market 40
5. SOCIAL SYSTEM: Communicability Network for Authors of Korean Meteorological Society 45

Ⅳ. Conclusion **49**

Ⅴ. Reference **53**

List of Figures and Tables

1. BIOLOGICAL SYSTEM: Protein Contact Network of Amino Acid

Fig. 1.1: Degree distributions of the α (circle), β (triangle), $\alpha+\beta$ (square), and α/β (diamond) groups 22

Fig. 1.2: Averaged shortest path length L as a function of the number of nodes N plot for each group with logarithmic scales 23

Fig. 1.3: (a) Local clustering coefficient C_l for each group scale logarithmically with N. (b) Global clustering coefficient C_g for each group scaled logarithmically with N 23

Fig. 1.4: Assortative coefficient r of the four protein groups as a function of N 25

Fig. 1.5: Modularity Q as a function of N 25

Fig. 1.6: (a) Global efficiency E_g and (b) local efficiency E_g for the four gropes of proteins and random controls 26

2. GEOLOGICAL SYSTEM: Seismic Network of California in USA

Fig. 2.1: Degree distribution as a function of degree k 28

Fig. 2.2: Characteristic path length as a function of cell width 29

Fig. 2.3: Mean clustering coefficient as a function of cell width 29

Fig. 2.4: Small-worldness as a function of cell width 30

Fig. 2.5: Cost efficiency as a function of cell width 30

Fig. 2.6: Global efficiency as a function of cell width 31

Fig. 2.7: Modularity as a function of cell width 31

Fig. 2.8: Assortativity as a function of cell width 32

3. GEOLOGICAL SYSTEM: Seismic Network of Japan

Fig. 3.1: Degree distribution as a function of degree k 34

Fig. 3.2: Plot of the mean degree as a function of cell width 34

Fig. 3.3: Characteristic path length versus as a function of cell width 35

Fig. 3.4: Mean clustering coefficient as a function of cell width 35

Fig. 3.5: Small-worldness as a function of cell width 36

Fig. 3.6: Cost efficiency as a function of cell width 36

Fig. 3.7: Global efficiency as a function of cell width 37

Fig. 3.8: Plot of the assortativity as a function of cell width 37

Fig. 3.9: Modularity as a function of cell width 38

4. ECONOMIC SYSTEM: Visibility Network of Korea Stock Market

Fig. 4.1: Degree distribution of the KOSPI data (top) and the triangle the KOSDAQ data (down) versus as a function of k 42

Fig. 4.2: Global efficiency as a function of the node 43

Fig. 4.3: Modularity as a function of the node 43

Fig. 4.4: Assortative coefficient as a function of the node 44

5. SOCIAL SYSTEM: Communicability Network for Authors of Korean Meteorological Society

Fig. 5.1: Color map diagram of relative communicability function matrices G_{pq}^{RA} (top) and G_{pq}^{EL} (down) for major 500 members of the author network 46

Fig. 5.2: Values of averaged communicability functions, G_p^{EA}, G_p^{RA}, G_p^{EL}, and $1/G_p^D$ for four beta values 47

Table 2.1: Numerical computation of statistical quantities performed from seismic time series data taken in southern California of USA 28

Table 3.1: Numerical computation of statistical quantities performed from seismic time series data taken in Japan 33

Table 4.1: Numerical computation of statistical quantities performed from (a) the KOSPI and (b) the KOSDAQ 41

Table 5.1: Values of the averaged communicability functions and the weight of community (W_C) 45

I. INTRODUCTION

1. BIOLOGICAL SYSTEM: Protein Contact Network of Amino Acid

In past two decades, many researches have been provoked considerable interest in complex systems. Network has emerged as a crucial framework in biological networks, when researchers study and analyze an open and novel problem in complex systems [1-7]. The most important properties of biological networks are the structural and topological ones involving interacting amino acids. Biological systems have been simulated and analyzed in networks such as the protein-protein interaction network [8], metabolic pathways network [9,10], gene regulatory network [11], and protein as a network of amino acids [12-15].

There have been many researches involving studying proteins as networks. In the biological network, when we consider that cellular networks are governed by universal laws and offer a new conceptual framework, the degree distribution follows a Poisson distribution or a power-law distribution. The degree distribution in random network follows a Poisson distribution, which indicates that most nodes have roughly the same number of links, approximately equal to the network's average degree [16]. In contrast, a scale-free network has a power-law degree distribution, $p(k) \sim k^{-\gamma}$, with a scaling exponent γ. In the case of $2 < \gamma < 3$, a few hubs bind numerous small nodes and the hubs may play a crucial role in the network. Recent published papers have claimed that the protein-protein interaction networks have the characteristics of a scale-free network [17-20]. In scale-free networks, most proteins can be involved in only on a few interactions, while a small set of hubs relate to dozens of interactions.

There have been several published works concerning proteins in biological networks. Vendruscolo et al. [13] showed that protein structures have a small-world network. They also identified that the key residues in the ensemble structures play the key role of hubs in the network of interactions to stabilize the structure of the transition state. In the short-range and long-range interaction networks in protein structures, Greene and Higman [14] calculated that the long-range interaction network is not a small world. They also showed that its degree distribution has a scale-free behavior indicative of a single-scale system. Atilgan et al. [15] investigated the topological properties of the network in the core and surface of globular protein size; the cores have the same local packing arrangements. Through example of a binding protein, they refined how the small-world network is useful in the efficient and eff ective dissipation of energy generated upon binding.

In this work, the network analysis of protein structures is treated to understand and assess the possible relevance of various parameters. We study the robustness of the topological properties of a biological network with various parameters. We treat the structural classification across four major groups (e.g., α, β, $\alpha+\beta$, α/β groups.) as enumerated in the Structural Classification of Proteins (SCOP) [21]. We mainly estimate global network metrics such as the averaged shortest path length, averaged clustering coefficient, local efficiency, global efficiency, assortative coefficient, and modularity. These parameters constitute the structural framework of proteins and provide the features of protein networks.

2. GEOLOGICAL SYSTEM: Seismec Network of California in USA

Recently, the complex system [1-3,22] has recently been applied to research new methods and high techniques in various scientific fields such as the intermittent nature of turbulence [23-25], the various financial time series [26,27], the wavelet transform approaches [28,29], the growing and non-growing networks [30,31], and the seismic phenomena [32], and so on. For the last two decades, the remarkable potential of complex networks to simulate and analyze the dynamical behavior of complex systems has gradually been an increasing trend in new fields of research in the social, natural, engineering, and medical sciences. In network theory, the small-world and scale-free network models [33] have been studied widely in various applications of the scientific fields. The two network models have played a crucial role in complex phenomena [34-36]. Of the many systems of current interest, the degree distribution for scale-free networks, is interesting because it follows the power law and for random networks it decays faster than exponentially. In a biological network, recent published papers have claimed that the protein-protein interaction networks have the characteristics of a scale-free network [36-39]. In scale-free networks, most proteins can deliberate only on a few interactions, while a small set of hubs relate to dozens of interactions.

Seismicity is a phenomenon of the dynamical behaviors in complex seismic time series [38-41], similar to a tsunami wave train. The shallow earthquake is well known to reorganize and analyze the distribution in the relevant area that leads to many aftershocks [38,42-46]. Furthermore, network theory is a topologically and dynamically useful tool for investigating and analyzing a seismic system, which can be simplified as processes for storing and transmitting energy via the crust. Abe and Suzuki [30,31] have discussed the novel method, which uses the concept of complex networks, and small-world and scale-free networks, for seismic complexity. Abe and Suzuki also introduced a complex-network approach [47] to the seismicity, and they showed that the earthquake network behaves like a complex network. Peixoto and Prado applied the complex network approach to a self-organized criticality model. They showed that a scale-free network was, in fact, realized by the model under certain conditions in the oceanic problems [35,36]. Recently, Baek et al. studied the seismic network by considering the cell resolution and the temporal causality based on seismic activity data for the Korean peninsula [39]. They mainly estimated and analyzed several global network metrics.

In this work, we study the topological robustness of the seismic network against the spatial shift and the scale in a volume (equal to cubic cell) which is located on a tectonic plate without boundaries. We mainly estimate the global network metrics such as the probability distribution of degree, characteristic path length, mean clustering coefficient, small-worldness, cost efficiency, global efficiency, modularity, and assortative coefficiency from the seismic data of southern California of USA.

3. GEOLOGICAL SYSTEM: Seismic Network of Japan

Complex system has recently been applied to research new methods and high techniques [48-51] in various scientific fields such as the intermittent nature of turbulence [23,25], the various financial time series [26,27], the wavelet transform approaches [28,29], the growing and non-growing networks [30,31], and the seismic phenomena [32], and so on. For the last two decades, the remarkable potential of complex networks to simulate and analyze the dynamical behavior of complex systems has gradually been an increasing trend in new fields of research in the social, natural, engineering, and medical sciences. The seismic phenomena in the network systems have performed diverse functions and also provided structural basis in the crust of earth. Characteristically, the network metrics of the seismicity may be supported to understand possible relevance of various seismic phenomena. The universal and irregular properties of statistical quantities in seismic network do not find unambiguously as yet, and this is an open problem that comes to a settlement.
In network theory, the small-world and scale-free network models [37] have been studied widely in various applications of the scientific fields. The two network models have played a crucial role in complex phenomena. For the many systems of current interest, the degree distribution for scale-free network, is interesting because it follows the power law and for random networks it decays faster than exponentially. In a biological network, recent published papers have claimed that the protein-protein interaction networks have the characteristics of a scale-free network [38,39]. In scale-free networks, most proteins can deliberate only on a few interactions, while a small set of hubs relate to dozens of interactions.

Seismicity is a phenomenon of the dynamical behaviors in complex seismic time series [40,41], similar to a tsunami wave train. The shallow earthquake is well known to reorganize and analyze the distribution in the relevant area that leads to many aftershocks [38,43-46]. Furthermore, network theory is a topologically and dynamically useful tool for investigating and analyzing a seismic system, which can be simplified as processes for storing and transmitting energy via the crust.

Several authors [47,52,53] have tested the validity of seismic model by simulating specific configurations that are analytic methods to complex networks. That is, Abe and Suzuki have discussed and analyzed the method, which uses the concept of small-world and scale-free networks for seismic complexity. Abe and Suzuki also introduced a complex-network approach [47] to the seismicity, and they showed that the earthquake network behaves like a complex network. Peixoto and Prado [54,55] applied the complex network approach to a self-organized criticality model. They showed that a scale-free network was, in fact, realized by the model under certain conditions in the oceanic problems. Recently, Baek et al. [53] studied the seismic network by considering the cell resolution and the temporal causality based on seismic activity data for the Korean peninsula [53]. They mainly estimated and analyzed several global network metrics. The detection of statistical quantities within seismic networks is an open subject of great interest for the unknown dynamics governing seismicity as yet.

In this work, we study the topological robustness of the seismic network against the spatial shift and the scale in a cubic cell which is located on a tectonic plate without boundaries. We mainly estimate the global network metrics such as the probability distribution of degree, characteristic path length, mean clustering coefficient, small-worldness, cost efficiency, global efficiency, modularity, and assortativity, from the seismic data of Japan.

4. ECONOMIC SYSTEM: Visibility Network of Korea Stock Market

In the past time, complex systems are usually distinct from the interacting and structural systems described by the periodic lattices in Euclidean space in many aspects. Scientists have recognized that the graph or network for complex systems has an intriguing structure and its peculiar property. Complex system has recently been applied to research new methods and high techniques [1,56-58] in various scientific fields such as the intermittent nature of turbulence [23-25], the various financial time series [26,27], the wavelet transform approaches [28,29], the growing and non-growing networks [30,31], and the seismic phenomena [32], the protein-protein interactions [37], and so on. The remarkable potential of complex networks to simulate and analyze the dynamical behavior of complex systems has been diffusively and rapidly an increasing trend in fields of research such as the social, natural, engineering, and medical sciences. For resent ten years, the visibility graph has provided a tool in time series analysis of diverse properties and structures mapping into in a network system. This network has inherited several properties and structures of time series and its investigation has revealed nontrivial information about the data of time series. Characteristically, the network metrics are able to be supported to understand and analyze the possible relevance of various natural phenomena.

In network theory, the small-world and scale-free network models have been studied widely in various applications of the scientific fields. The two network models have played a crucial role in complex phenomena. Of the many systems of current interest, the degree distribution for scale-free networks, is interesting because it follows the power law and for random networks it decays faster than exponentially.

In recent years, the current economic crisis calls for a deeper understanding of the dynamics of economic activities on the global economic network [59]. The studies in this field can be classified into two types based on how the network is constructed. The studies of the first type deal with many time series to form a complex network with each node standing for a time series and the weight of a link between two nodes characterized by the correlation coefficient of the two time series [60-62] or by the distance between the two time series [63,64].

Concerning the studies of the second type, different mapping methods have been proposed to convert time series into different kinds of networks, including cycle networks based on the local extrema and their distance in the phase space [65,66], segment correlation networks [67,68], nearest neighbor networks [69], n-tuple networks based on the fluctuation patterns [70,71], the visibility of nodes [72], space state networks based on conformational fluctuations [73], and bin transition networks [74], and recurrence networks. The visibility algorithm has been diversely used to investigate stock market indices [75], human strive intervals [76], occurrence of hurricanes in the United States [77], foreign exchange rates [78], and energy dissipation rates in three-dimensional fully developed turbulence.

5. SOCIAL SYSTEM: Communicability Network for Authors of Korean Meteorological Society

Network science has emerged and been utilized as one of the important frameworks when each researcher studies complex systems [1-3,5,58,79,80]. An important property of networks is the existence of modules or communities, and the communicability between a pair of nodes in a network is concerned with the shortest path connecting both nodes. Estrada et. al. [81] proposed a generalization of the communicability by elucidating both for the shortest paths communicating between two nodes and for all the other walks travelling between two distances. The communicability detection allows one to determine potentially the unaware and hidden relationships between nodes and also allows one to reduce a large complex network into smaller and smaller groups. Presently, the community detection within networks is an open subject of great interest. Complex networks are also ubiquitous in many biological, ecological, technological, informational, and infrastructural systems [4,41,82-86]. It is clear that the atomic, oscillating, and social systems display network-like structures using the tools of statistical mechanics. These methods and techniques were contributed to shed light on the structure and dynamics of social, economic, biological, technological, and medical systems [87-89]. It is actually recognized that the analogy functions that describe the properties depend mainly on the structural properties of the system in networks as well.

Recently, an important issue in regards to networks has recently been the cascade effect in both the ecological network and the multiplex network. The former propagates well beyond the nearest neighbors of the extinguished species [90-92] with protein–protein interactions. The latter describes the fact that multiplex structures with different strength of coevolution respond differently to the cascade process, exemplifying the dynamical signature that coevolution can imprint [93].

In this paper, we study the community structure of the Korean meteorological society in the author network. The data we used are the published papers of 1,943 authors from the Korean meteorological society publications in the author network, from March 2008 to November 2013. We simulate and analyze four other kinds of averaged communicability indices such as G_p^{EA}, G_p^{RA}, G_p^{EL}, and $1/G_p^{D}$.

II. METHODOLOGY

1. General Network Properties

Since the degree k_i of a node i is the number of nodes to which it is directly connected, the average degree k of a network with N nodes is defined as

$$k = \frac{1}{N}\sum_{i=1}^{N} k_i. \tag{1}$$

The averaged shortest path length(characteristic path length) is defined as

$$L = \frac{2}{N(N-1)}\sum_{i=1}^{N-1}\sum_{j=1}^{N} L_{ij}, \tag{2}$$

where L_{ij} is the shortest path length between nodes i and j. We consider that diameter of the network is the largest of all the shortest path lengths. If the averaged shortest path length or the diameter is proportional to $\log N$, it can be ascertained that the properties of a network satisfy the small-worldness. Furthermore, a network has a small averaged clustering coefficient and having degree distribution of a power-law form is known as the scale-free network [94].

The global clustering coefficient C_g is defined as the transitivity ratio, i.e., the fraction of the closed triplets to whole triplets. That is

$$C_g = \sum \frac{\text{no. of closed triplet}}{\text{no. of triplet}} = \sum \frac{3 \times \text{no. of triangle}}{\text{no. of triplet}}. \tag{3}$$

In another view point, the averaged clustering coefficient C_l is calculated as

$$C_l = \frac{1}{N}\sum_{i=1}^{N} C_i. \quad (4)$$

Here, the clustering coefficient C_i for a node i is defined as the fraction of links that exist among its nearest neighbor nodes to the maximum number of possible links among them. That is

$$C_i = \frac{\text{no. of linked nearest neighbours}}{k_i(k_i - 1)/2} \quad (5)$$

A network is a small-world network if it has a large value of the averaged clustering coefficient and if its averaged shortest path length scales $\log N$ [86]. As another method for measuring the small-worldness, we can compute the small-worldness S_w using the Eqs. (2) and (3), or Eqs. (2) and (4) as

$$S_w = \frac{C/C_{rand}}{L/L_{rand}}, \quad (6)$$

where C_{rand} and L_{rand} are, respectively, the mean clustering coefficient and the characteristic path length of a random network constructed by randomizing the empirical network under fixed links and nodes. The value in Eq. (6) is greater than unity for a small-world network.

On the other hand, the global efficiency of networks is defined as follows. We introduce the global efficiency E_g [95] as

$$E_g = \frac{2}{N(N-1)}\sum_{i=1}^{N-1}\sum_{j=i+1}^{N}\frac{1}{L_{ij}}. \quad (7)$$

In contrast that the characteristic path length is the averaged shortest path length in Eq. (2), the global efficiency is averaged reciprocal of the shortest path length. Thus if there are many pairs that their shortest path lengths are large, the efficiency is small.

As we consider a network for the neighbors of node i, the local efficiency E_l becomes the averaged value of the global efficiencies of the nearest neighbors of node i as

$$E_l = \frac{1}{N}\sum_{i=1}^{N} E_i. \tag{8}$$

Also, the cost efficiency is defined as

$$C_e = \frac{E_{\text{total}}}{E_{\text{possible}}}, \tag{9}$$

where E_{total} and E_{possible} are the total number of edges (links) and the number of all possible edges, i.e., $E_{\text{possible}} = N(N-1)/2$ for N nodes network, respectively.

Now, the assortative coefficient is the Pearson correlation coefficient of the degrees at either end of a link measures the tendency of degree correlation. The assortative coefficient r is defined [96] as

$$r = \frac{1}{\sigma_q^2}\sum_{i=1}^{N}\sum_{j=1}^{N} ij(e_{ij} - q_i q_j), \tag{10}$$

where $q_i = (i+1)p_{i+1}/\sum_{n=1}^{N} np_n$. The index i and j are the degrees of nodes, q_i and q_j are the remaining degree distributions, e_{ij} is the joint distribution of the remaining degrees of the two nodes at either end of a randomly chosen link, and σ_q^2 is the variance of the distribution q_j. The assortative coefficient presents the tendency of connectivity of high-degree nodes. This means the correlation coefficient of remaining degree distributions that take a value between -1 and 1. The assortative coefficient is negative in general networks if a high degree node tends to connect low degree nodes.

Lastly, modularity is a value of a community structure that is the number of edges falling within groups minus the expected number in an equivalent network with edges placed at random [97]. This is represented in terms of

$$Q = \frac{1}{4m} \sum_{i=1}^{N} \sum_{j=1}^{N} \left(A_{ij} - \frac{k_i k_j}{2m} \right) s_i s_j, \qquad (11)$$

where $s_i = 1$ if the node i exists in a group, and $s_i = -1$ if the node i does not exist in another group. The quantity A_{ij} is the number of edges between vertices i and j it will normally be 0 or 1, although the larger values are possible in networks where the multiple edges are allowed. The expected number of edges between i and j if the edges are placed at random is $k_i k_j / 2m$, where k_i and k_j are the degrees of the vertices, and is the total number of edges in the network.

From Eqs. (1) - (11), we simulate and analyze the topological measures of a complex network in next section. These mathematical techniques can be employed in the empirical investigation of diverse models.

2. Protein Contact Network in Biological System

In this section, we introduce the topological properties of networks in the structural classification of proteins. First of all, we explain two coarse-grained models of protein structure controls that are manipulated in our studies as follows: we model the native-state protein structure as a network consisting of its constituent amino acids and their non-covalent interactions. The Protein Contact Network (PCN) is a graph-theoretical representation of protein structure, in which each amino acid is a node and the spatial proximity of any two amino acids is a link between them. Any two amino acids are considered to be in a spatial contact if the distance between their atoms was less than or equal to the value of 8Å selected in our case. We may select these distances to be less than or equal to 5Å, 6Å, or 7Å arbitrarily [13-15] in other future researches [98]. The choice of distances can be based on the range at which non-covalent interactions are effectively responsible for the polypeptide chain to fold into its native state.

3. Seismic Network in Geological System

We mainly consider the theoretical background of the various global network metrics. First of all, in order to construct a seismic network, we consider a network by segmenting the whole region into three-dimensional cells (cubes) and making a link between consecutive events. Each cell is regarded as node of a network, and the network constructed in that manner is basically directed, but we transform it into an undirected one because we focus on the topology of the network. The procedure is as follows:

(Ⅰ) Segment the whole region into cubic cells, each of which has the same size.
(Ⅱ) Link two earthquakes occurring consecutively.
(Ⅲ) If two consecutive events belong to the same cell, their link is disregarded.
(Ⅳ) If two directed links form between two cells, the number of links is counted as one [32].
(Ⅴ) By considering each cell as a node, we regard the links made by all events belonging to the cell with others in another cell as links of a network.

4. Visibility Network in Economic System

In this work, we study to which extent the method and its technique of visibility graph theory are useful as a way to characterize time series of the KOSPI and the KODAQ in Korean financial markets. We mainly estimate the important global network metrics such as the global efficiency, the modularity, the assortativity, and so on, and we perform the numerical calculation and its analysis.
In financial networks, we construct the visibility network according to the following

prescriptions: (1) We firstly connect each node seeing at least its nearest neighbors (left and right). (2) There is no direction defined in the links as the way that the algorithm is built up. (3) Lastly, under affine transformations of the series data, the visibility criterion is invariant under rescaling of both horizontal and vertical axes, and under horizontal and vertical translations. In a financial market, we recall the visibility criteria [72] as follows: two arbitrary data values of a stock market index $P(t_i)$ and $P(t_j)$ will have visibility, and consequently will become two connected nodes of the associated graph, if any other data $P(t_k)$ placed between them fulfills. That is, the relation is given by

$$\frac{P(t_k)-P(t_j)}{t_k-t_j}<\frac{P(t_i)-P(t_j)}{t_i-t_j}. \tag{12}$$

It is well known that the visibility graph of a time series remains invariant under several transformation of the time series. The original time series with visibility links present as the translation of the data, the vertical rescaling, the horizontal rescaling, and the addition of a linear trend to the data. Hence, the visibility graphs for all these cases remain invariant.

5. Network Communicability in Social System

In this section, we mainly consider the theoretical methods of microscopic communicability in networks. First of all, let us introduce the concept of communicability in networks by describing a community structure. The communicability structure can invoke the concept of walks in networks. A walk of length k is a sequence of nodes n_0, n_1, ..., n_k such there is a link from n_{i-1} to n_i for each $i=1, 2, \ldots, k$ [99]. Using the concept of walk we can define the communicability between two nodes. That is, the communicability between the nodes p and q in a network is the weighted sum of all walks starting at node p and ending at node q, in which the weighting scheme gives more weight to the shortest walks than to the longer ones. The communicability function [80] is represented in terms of

$$G_{pq} = \sum_{k=0}^{\infty} c_k \left(A^k\right)_{pq}. \tag{13}$$

Here, A is the adjacency matrix, which has unity if the nodes p and q are linked to each other, but has zero otherwise. The adjacency matrix $\left(A^k\right)_{pq}$ gives the number of walks of length k starting at the node p and ending at the node q [100,101]. The two novel communicability functions are calculated as

$$G_{pq}^{EA} = \sum_{k=0}^{\infty} \frac{\left(A^k\right)_{pq}}{k!} = \left(e^A\right)_{pq} \tag{14}$$

and

$$G_{pq}^{RA} = \sum_{k=1}^{\infty} c_k \left(W^k\right)_{pq} = \sum_{k=1}^{\infty} \alpha^k \left(W^k\right)_{pq} = (I - \alpha W)^{-1}, \tag{15}$$

where e^A is a matrix function that can be defined using the following Taylor series [102]. The communicability function G_{pq} is obtained by using the weighted adjacency matrix $W = \left(W_{ij}\right)_{n \times n}$. Centrality measures were originally introduced in social sciences [103,104] and are now widely used in the whole field of complex network analysis [83].

First of all, let us consider every node as one oscillator of mass m and every link as a spring with the spring constant $m\omega^2$ connecting two oscillators. The oscillator network is submerged into a thermal bath at the temperature T, and then the oscillators in the complex network oscillate under thermal disturbances. We introduce a Hamiltonian of the oscillator network such as

$$H_A = \sum_{i=1}^{n} \left[\frac{p_i^2}{2m} + \frac{m\omega^2}{2}(K - k_i)x_i^2 \right] + \frac{m\omega^2}{2} \sum_{i,\, j}^{n} A_{ij}(x_i - x_j)^2, \qquad (16)$$

where k_i is the number of links that are connected to the node i and K is a constant satisfying $K \geq \max k_i$. The first term of the right-handed side takes two terms as both the kinetic energy of the oscillator i and a counter term that offsets the movement of the network as a whole by tying the network to the fat. The second term of the right-handed side is the potential energy of the springs connecting the oscillators, because $x_i - x_j$ is the extension or the contraction of the spring connecting the nodes i and j.

Instead of the Hamiltonian H_A in Eq. (16), let us next reconsider the Hamiltonian of the oscillator network in the form

$$H_L = \sum_{i=1}^{n} \frac{p_i^2}{2m} + \frac{m\omega^2}{2} \sum_{i,\, j}^{n} A_{ij}(x_i - x_j)^2. \qquad (17)$$

Because the Hamiltonian H_L lacks the springs that tie the whole network to the flat, this network can undesirably move as a whole. Next, we can expand Eq. (17) as

$$\begin{aligned} H_L &= \sum_{i=1}^{n} \left(\frac{p_i^2}{2m} + \frac{m\omega^2}{2} k_i x_i^2 \right) - \frac{m\omega^2}{2} \sum_{i,\, j}^{n} x_i A_{ij} x_j \\ &= \sum_{i=1}^{n} \frac{p_i^2}{2m} + \frac{m\omega^2}{2} \sum_{i,\, j}^{n} x_i L_{ij} x_j, \qquad (18) \end{aligned}$$

where L_{ij} denotes an element of the network Laplacian L. This is often used in analyzing diffusion phenomena on complex networks.

In the network of classical oscillators, we consider the Hamiltonian of the form as

$$H_A = \frac{Km\omega^2}{2}\sum_{i=1}^{n} x_i^2 - \frac{m\omega^2}{2}\sum_{i,\,j}^{n} x_i A_{ij} x_j$$

$$= \frac{m\omega^2}{2} x^T (KI - A)x, \tag{19}$$

where $x = (x_{1,}, x_{2,} \ldots, x_n)^T$ and I is the identity matrix. After arranging several processes, we can derive the communicability function as

$$G_{pq}^{RA} = \beta K m\omega^2 G_{pq}(\beta) \tag{20}$$

with the identification $\alpha = 1/K$. A correlation between two node displacements in a network is represented in terms of

$$G_{pq}(\beta) = \frac{1}{\beta K m\omega^2}(I - (A/K)^{-1}]_{pq}. \tag{21}$$

This represents a correlation between the node displacements in a network due to small thermal oscillations [105,106]. From the fact that the Laplacian matrix of a connected network has a non-degenerate zero eigenvalue, we can calculate another correlation function as

$$G_{pq}^{D}(\beta) = \frac{1}{\beta K m\omega^2}(L^+)_{pq}, \tag{22}$$

where L^+ is the Moore–Penrose generalized inverse of the Laplacian.

In a network of quantum oscillators, we start by considering the quantum-mechanical counterpart of the Hamiltonian H_A. With the use of several operators, we can recast the Hamiltonian in Eq. (16) into the form

$$H_A = \sum_{i=1}^{n} \hbar\Omega\left(a_i^+ a_i + \frac{1}{2}\right)x_i^2 - \frac{\hbar\omega^2}{4\Omega}\sum_{i,\,j}^{n}\left(a_i^+ + a_i\right)A_{ij}\left(a_j^+ + a_j\right). \tag{23}$$

We use the boson creation and annihilation operators defined by

$a_i^+ = \frac{1}{\sqrt{2\hbar}}\left(\sqrt{m\Omega}\, x_i - \frac{i}{\sqrt{m\Omega}} p_i\right)$ and $a_i = \frac{1}{\sqrt{2\hbar}}\left(\sqrt{m\Omega}\, x_i + \frac{i}{\sqrt{m\Omega}} p_i\right)$, where $\Omega = \sqrt{K/m\omega}$, and the commutation relation is given by $\left[a_i, a_j^+\right] = \delta_{ij}$. After arranging several equations, we can see that

$$G_{pq}^{EA} = \exp(\beta\hbar\Omega) G_{pq}^{A}(\beta) \tag{24}$$

The diagonal thermal Green's function is given in the framework of quantum mechanics, and we can compute the off-diagonal thermal Green's function as

$$G_{pq}^{A}(\beta) = \exp(-\beta\hbar\Omega)\left[\exp\left(\frac{\beta\hbar\omega^2}{2\Omega} A\right)\right]_{pq}. \tag{25}$$

Note that the constant K affects only the proportionality constant through $\Omega = K/m\omega$ in Eq. (25). This means that when the temperature tends to infinity or $\beta \to 0$, there is absolutely no communicability between any pair of nodes. That is, $G_{pq}^{EA}(\beta \to 0) = 0$. If we consider the case when the temperature tends to zero or $\beta \to \infty$, then there is an infinite communicability between every pair of nodes, i.e., $G_{pq}^{A}(\beta \to \infty) = \infty$. Furthermore, the communicability function gives

$$G_{pq}^{EL}(\beta) = G_{pq}^{L}(\beta) - 1, \tag{26}$$

where the same quantum-mechanical calculation by using the Hamiltonian H_L in Eq. (17) gives

$$G_{pq}^{L}(\beta) = \left[\exp\left(-\frac{\beta\hbar\omega^2}{2\Omega} L\right)\right]_{pq}. \tag{27}$$

From Eqs. (26) and (27), the communicability function G_p^{EL} gives $G_{pq}^{L}(\beta) - 1$ upon setting $\beta\hbar\omega^2 = 2\Omega$ [80]. Lastly, we simulate and analyze the averaged communicability function [80] for a given node defined as

$$G_p = \frac{1}{n-1}\sum_{p \neq q}^{n} G_{pq}. \tag{28}$$

Consequently, from Eqs. (19) and (21), the communicability functions G_{pq}^{RA} and G_{pq}^{D} become the types of the thermal Green's function of classical harmonic oscillators in networks of the community structure. The communicability functions $G_{pq}^{EA}(\beta)$ and $G_{pq}^{EL}(\beta)$ also become the types of the thermal Green's function in quantum harmonic oscillators from Eqs. (24) and (26). We will make use of communicability functions to compute the measures of a community structure, and these mathematical techniques will lead us to more general results. In the subsequent section, we will simulate and analyze four other kinds of averaged communicability functions such as G_p^{EA}, G_p^{RA}, G_p^{EL}, and $1/G_p^{D}$.

III. RESULTS OF NETWORK PROPERTIES IN SCIENTIFIC PHENOMENA

1. BIOLOGICAL SYSTEM: Protein Contact Network of Amino Acid

We introduce the native-state protein structure as a network consisting of its constituent amino-acids and their interactions in the Structural Classification of Proteins [21]. The C atom of an amino acid has been used as a node and two such nodes are said to be linked if they are less than or equal to a threshold distance apart from each other [13,15], here we use 8Å as this threshold distance. It is well-known that proteins are composed predominantly of α helices and of β sheets. The $\alpha+\beta$ proteins mainly have anti-parallel β sheets, whereas α/β proteins consist of mainly parallel β sheets. We will treat the four structural classes of proteins as α, β, $\alpha+\beta$, and α/β in this paper. The structural classification across the four groups is enumerated in the Structural Classification of Proteins. The proteins that we consider consist of 2,879 α's, 2,786 β's, 3,491 $\alpha+\beta$'s, and 3,456 α/β's. The number of residues of each protein is from 27 to 10,432. The structural data is extracted from the Protein Data Bank (PDB) [107].

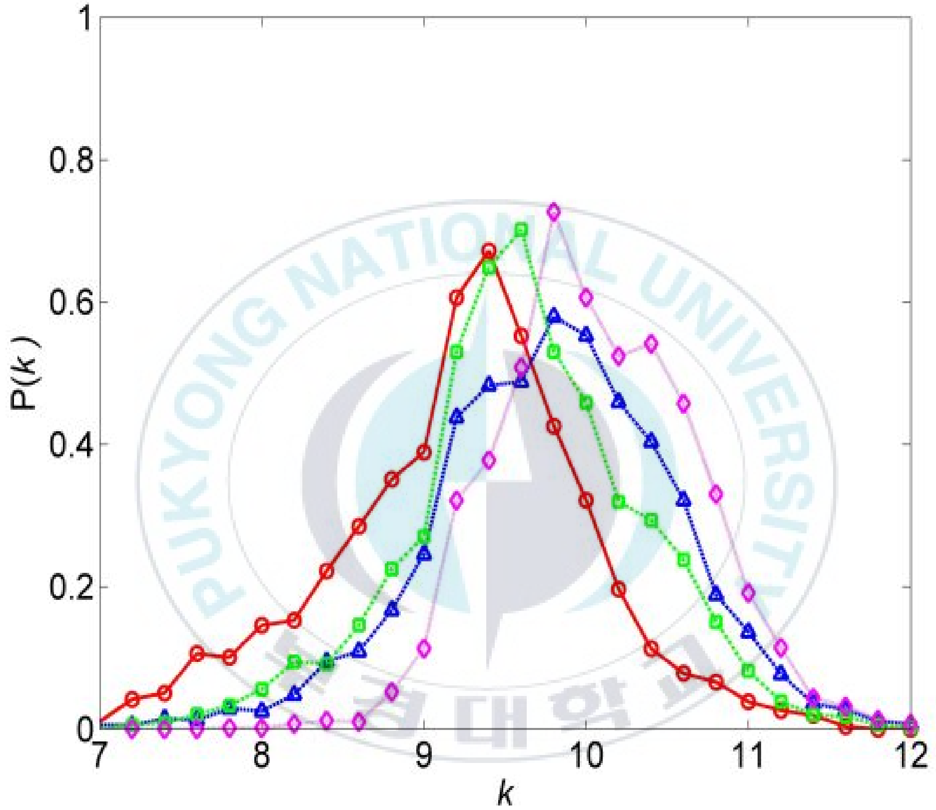

Fig. 1.1: Degree distributions of the α (circle), β (triangle), $\alpha+\beta$ (square), and α/β (diamond) groups. These functional forms have a uni-modal Poisson-like distribution.

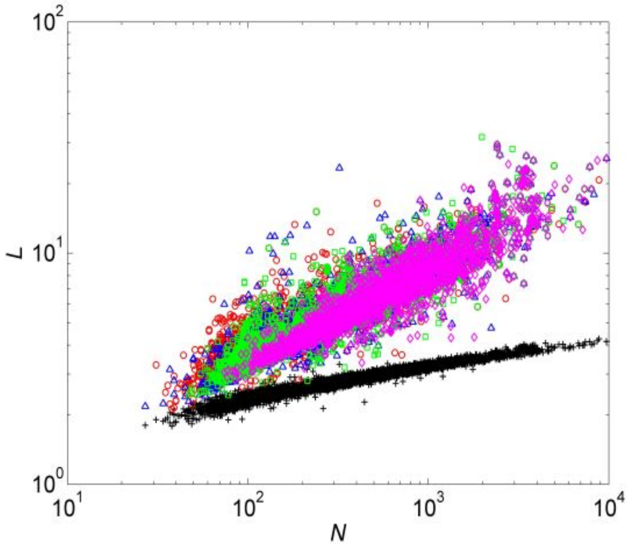

Fig. 1.2: Averaged shortest path length L as a function of the number of nodes N plot for each group with logarithmic scales. Here the circle, triangle, square, and diamond designate the α, β, $\alpha+\beta$, and α/β groups, respectively.

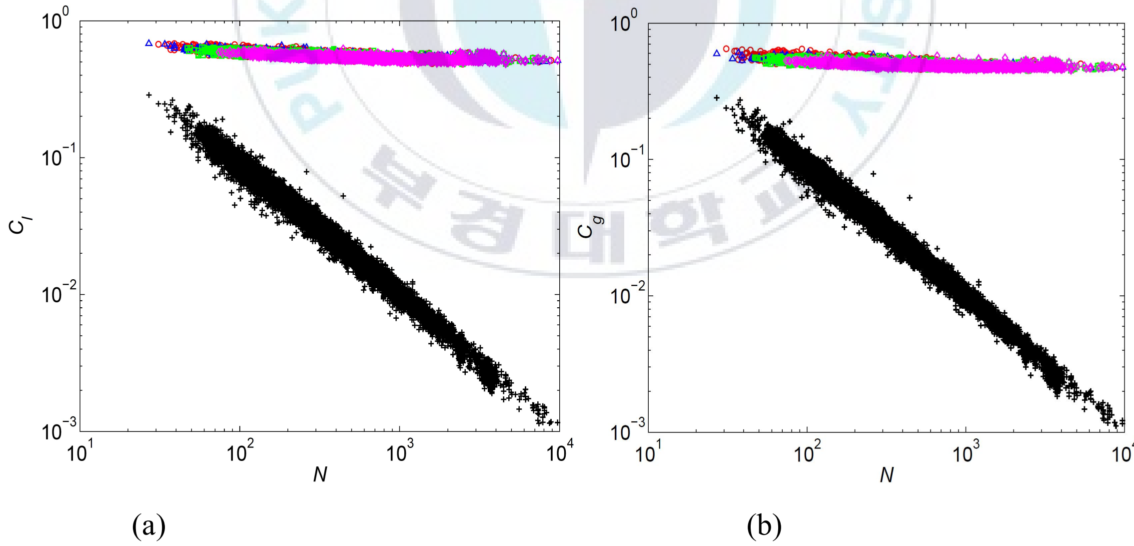

Fig. 1.3: (a) Local clustering coefficient C_l for each group scale logarithmically with N. (b) Global clustering coefficient C_g for each group scaled logarithmically with N. Here the circle, triangle, square, and diamond designate the α, β, $\alpha+\beta$, and α/β groups, respectively.

The distribution of the degrees is an important property which characterizes network topology. The degree distribution of a random network is presented by a Poisson distribution. **Figure 1.1** shows the degree distributions of α, β, $\alpha+\beta$, and α/β protein networks. These distributions are caused by the functional structure of the protein. The average degrees of the α, β, $\alpha+\beta$, and α/β groups are calculated as 9.23±0.81, 9.79±0.80, 9.62±0.72, and 10.06±0.65, respectively. The shape of these distributions is a bell-shaped Poisson form [14].

We calculate the averaged shortest path length L and its random graph for the observed proteins. **Figure 1.2** shows the averaged shortest path length L of four protein networks and of these random controls with logarithmic scales. We find that $\log L$ is approximately proportional to $\log N$ for four protein groups. It is furthermore ascertained from the random controls that the characteristic path length L is proportional to $\log N$. In this case we cannot represent that small-worldness as the characteristic path length has a large value.

We investigate the local and global clustering coefficients of the networks. **Figures 1.3(a)** and **1.3(b)** show that the clustering coefficients C_l and C_g of the proteins are larger values that those of the random controls. Since an averaged clustering coefficient characterizes the local organization, the C_l and C_g are expected to fall with increasing size [108] for both random controls. It is shown [15] that the C remains almost the same in the core of the protein regardless of size. A similar result [20] is shown for the metabolic networks of 43 distinct organisms. This property is suggestive of potential modularity in the topology of protein networks. The averaged local and global clustering coefficients are, respectively, 0.554±0.028 and 0.503±0.023 in the protein networks, while those for the random controls have values of 0.036±0.033. The Kolmogorov-Smirnov test [109] shows that the differences between C_l and C_g for the four gropes of proteins and random controls are statistically significant. Thus, the protein networks have significantly larger clustering coefficients rather than their random counterparts, and are found to make up small-world networks.

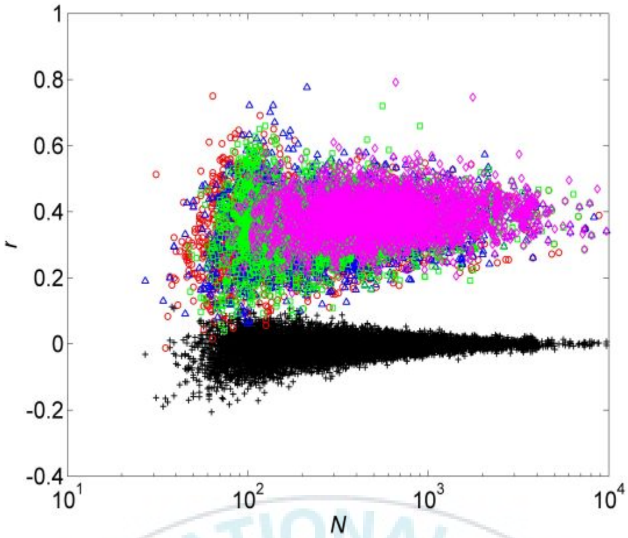

Fig. 1.4: Assortative coefficient r of the four protein groups as a function of N. Here the circle, triangle, square, and diamond designate the α, β, $\alpha+\beta$, and α/β groups, respectively.

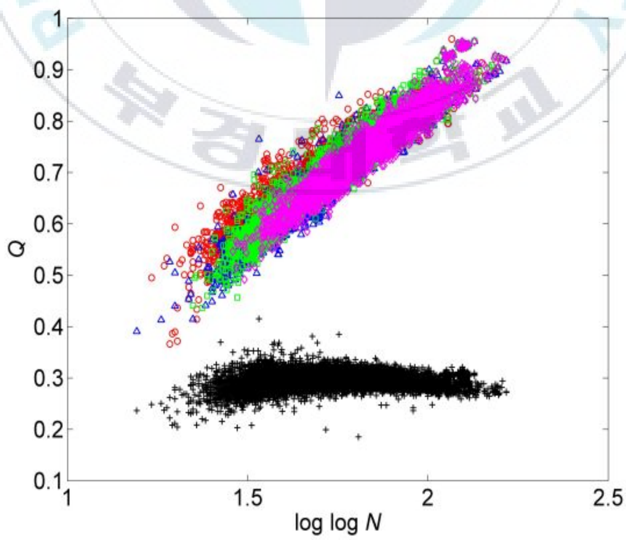

Fig. 1.5: Modularity Q as a function of N. Here the circle, triangle, square, and diamond designate the α, β, $\alpha+\beta$, and α/β groups, respectively.

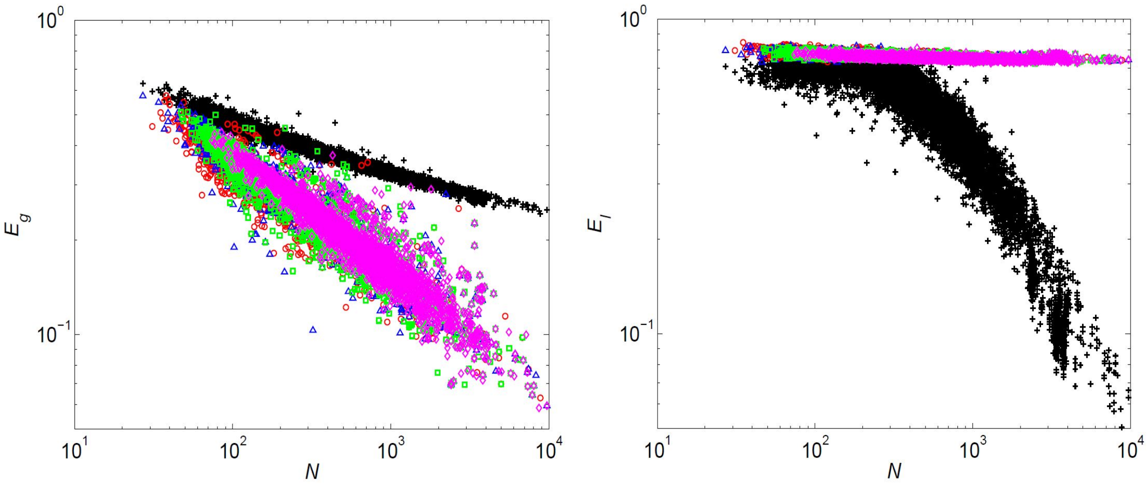

(a) (b)

Fig. 1.6: (a) Global efficiency E_g and (b) local efficiency E_g for the four gropes of proteins and random controls. Here the circle, triangle, square, and diamond designate the α, β, $\alpha+\beta$, and α/β groups, respectively.

Figure 1.4 shows the assortative coefficient of the four protein groups. Our assortative coefficient has positive values in the complex network. The averaged values of our proteins are approximately 0.361±0.082. **Figure 1.5** shows that the modularity Q increases as N increases. The values of the four groups are distinct from the random networks. In the random network, the modularity is almost constant as N increases. However, the modularity of the proteins is significantly large as an increasing function of N. The averaged values for the four protein groups and random controls are 0.726±0.097 and 0.296±0.014, respectively.

As shown in **Figure 1.6**, the averaged values as a function of N for the global and local efficiencies of each protein group are 0.235±0.084 and 0.763±0.014, respectively. On the other hand, the averaged values for the global and local efficiencies of random controls are 0.382±0.062 and 0.545±0.187, respectively. Thus we confirm that the local efficiencies are significantly large but the global efficiencies are significantly small based on the Kolmogorov-Smirnov test.

2. GEOLOGICAL SYSTEM: Seismic Network of California in USA

To discuss the earthquake networks based on the five years seismic data taken in southern California of the USA, the data source is the Advanced National Seismic System (http://www.ncedc.org/anss/catalog-search.html). The time interval is between 00:36:42 on the 1st of January 2006 and 23:55:30 in the 31th of December 2010. The region covered is 32°N - 42°N latitude and 114°W - 124°W longitude to the depth of 100 ㎞. Because we exclude artificial quarry blasts from the data, the data for the total numbers of events is 245,010 and contains only events with a magnitude larger than zero.

We construct an earthquake network by segmenting the whole region into three-dimensional cells and making a link between consecutive events. Each cell is regarded as node of a network, and the network constructed in that manner is basically directed, but we transform it into an undirected one because we focus on the topology of the network. The procedure is as follows: (1) we segment the whole region into cubic cells, each of which has the same size. (2) Link two earthquakes occurring consecutively. (3) If two consecutive events belong to the same cell, their link is disregarded. (4) If two directed links form between two cells, the number of links is counted as one. (5) By considering each cell as a node, we regard the links made by all events belonging to the cell with others in another cell as links of a network.

In order to examine the robustness of a network topology against spatial shifts and scales in volume, we simulate and analyze the regions between 3 km and 100㎞. We select several cell widths in **Table 2.1**, and the numerical computations for statistical quantities are typically performed from seismic time series data taken in southern California of USA. Moreover, the characteristic path length, mean clustering coefficient, global efficiency, modularity, and assortative coefficient for both our data's network and a random network is in fact compared and analyzed.

Table 2.1: Numerical computation of statistical quantities performed from seismic time series data taken in southern California of USA. Here, L_{rand}, C_{rand}, E_{rand}, Q_{rand}, and r_{rand} denote the characteristic path length, mean clustering coefficient, global efficiency, modularity, and assortative coefficient of a random network, respectively, and N denotes a number of nodes.

cell width (km)	N	C_e	$<k>$	L	L_{rand}	C	C_{rand}	S_w	E	E_{rand}	Q	Q_{rand}	r	r_{rand}
3	32,629	0.0003	10.415	3.142	4.694	0.259	0.0003	71.321	0.331	0.218	0.284	0.269	0.136	0.0002
6	13,964	0.0012	16.933	2.726	3.683	0.452	0.0013	38.746	0.384	0.279	0.196	0.211	0.136	0.0008
12	4,794	0.0061	29.226	2.447	2.836	0.635	0.0062	23.162	0.428	0.364	0.127	0.168	0.243	0.0041
24	1,248	0.039	48.524	2.124	2.107	0.765	0.039	8.743	0.492	0.495	0.082	0.127	0.374	0.0007
48	341	0.171	57.977	1.858	1.83	0.827	0.17	3.145	0.581	0.585	0.079	0.101	0.451	0.0014
96	95	0.45	42.295	1.551	1.55	0.852	0.45	1.617	0.725	0.725	0.068	0.086	0.412	-0.027

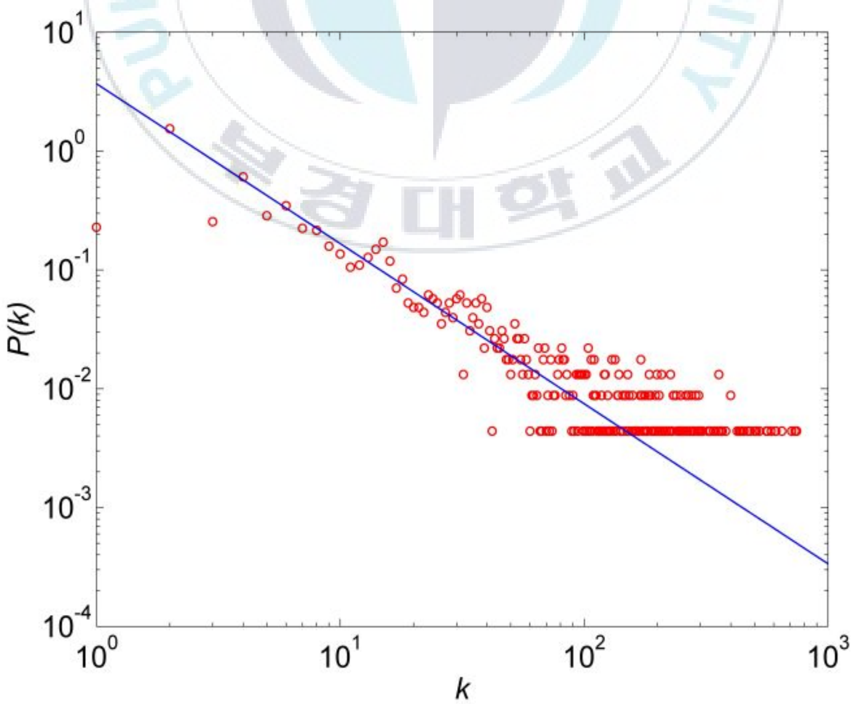

Fig. 2.1: Degree distribution as a function of degree k. The distribution follows a power-law with the slope is –1.35.

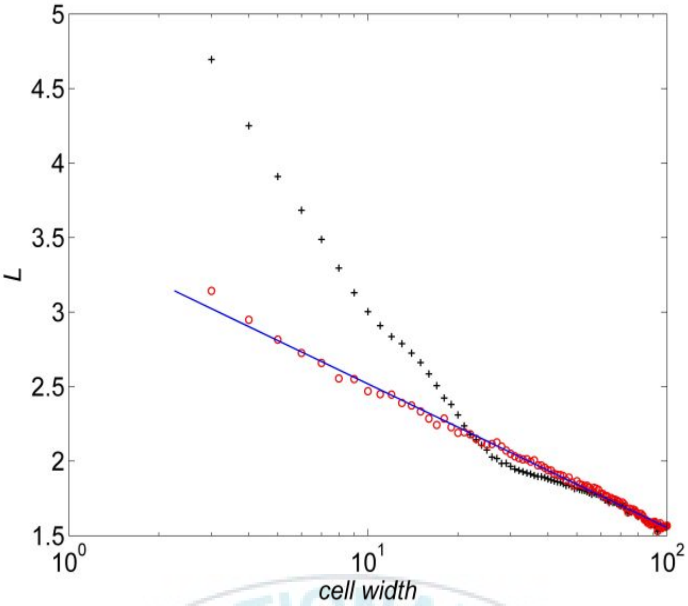

Fig. 2.2: Characteristic path length as a function of cell width, where the circle denotes the empirical data and the cross the random network. The slope (blue line) is –0.42.

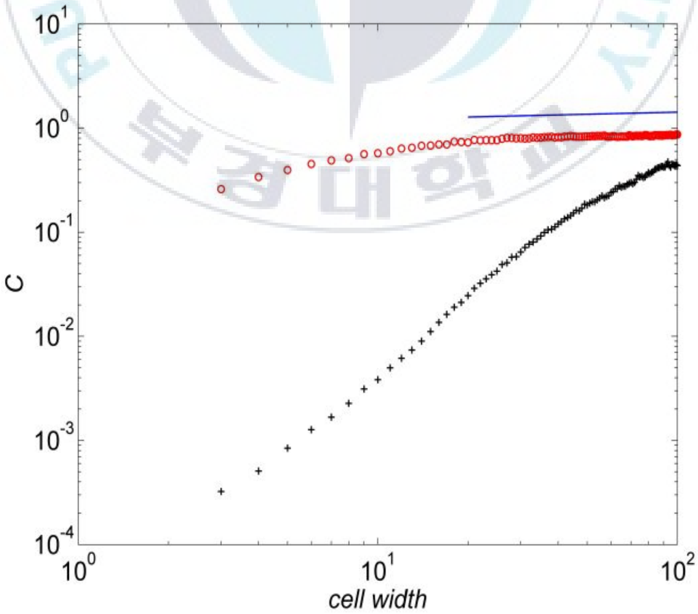

Fig. 2.3: Mean clustering coefficient as a function of cell width, where the circle denotes the empirical data and the cross the random network. The slope (blue line) is 0.07.

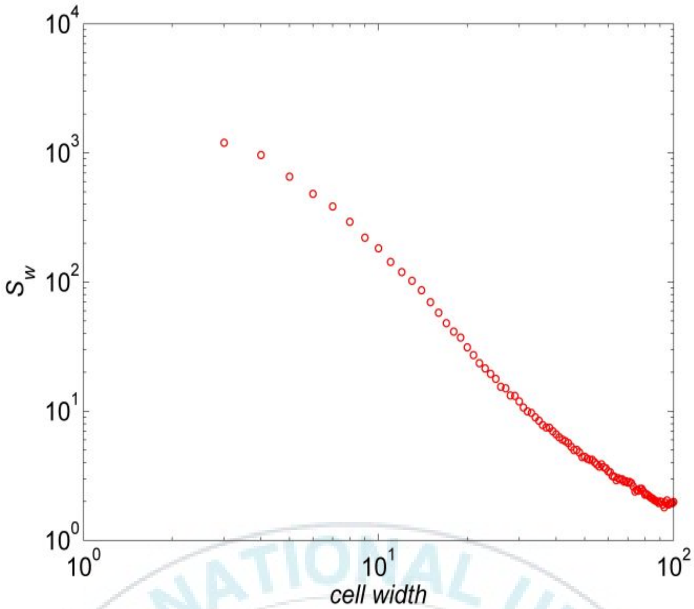

Fig. 2.4: Small-worldness as a function of cell width.

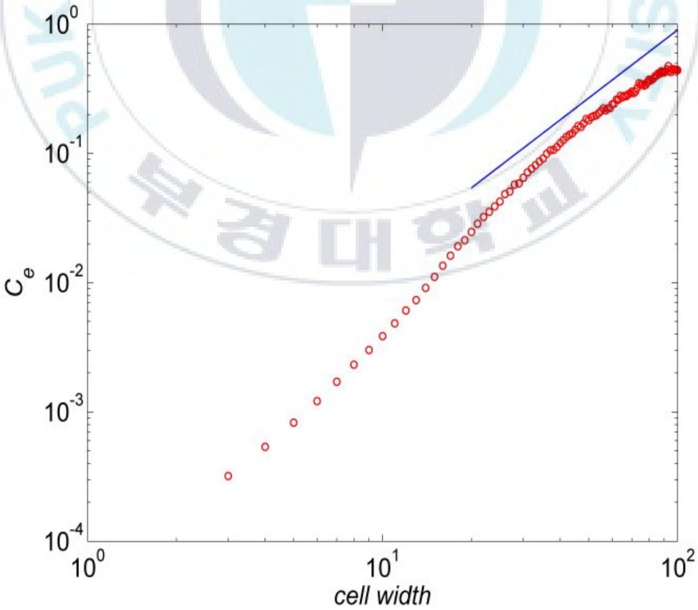

Fig. 2.5: Cost efficiency as a function of cell width, where the circle denotes empirical data and the cross the random network, and the value of slope (blue line) is 1.75.

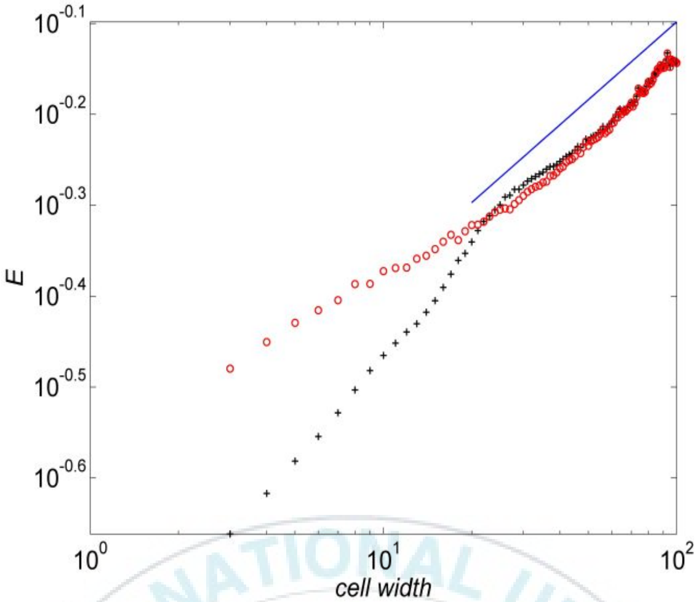

Fig. 2.6: Global efficiency as a function of cell width, where the circle denotes empirical data and the cross the random network, where the slope (blue line) is +0.28.

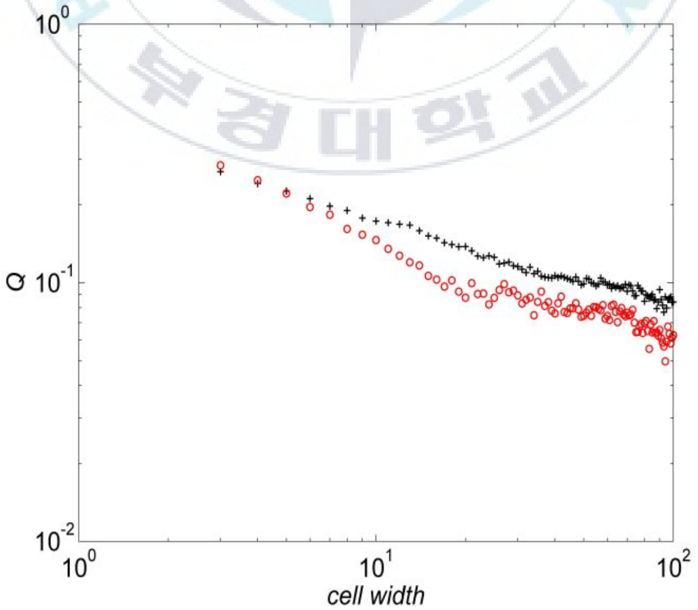

Fig. 2.7: Modularity as a function of cell width, where the circle denotes empirical data and the cross the random network.

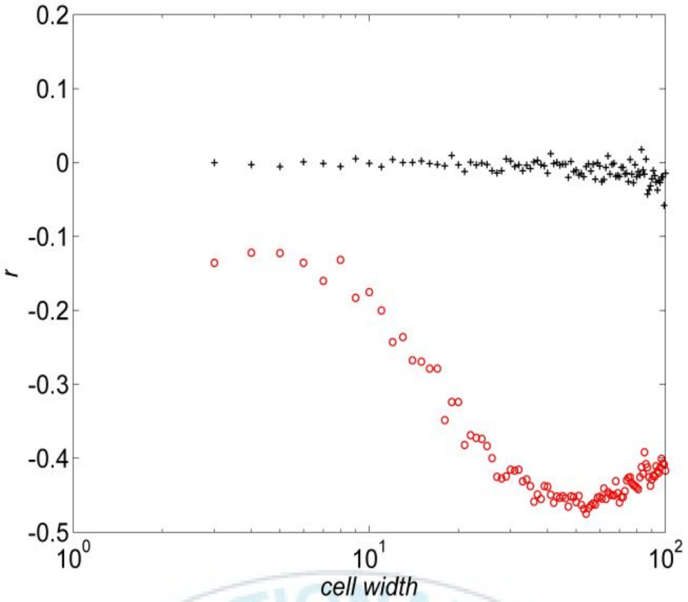

Fig. 2.8: Assortativity as a function of cell width, where the circle denotes our data and the cross the random network.

We typically perform the numerical computations for eight statistical quantities given by Eqs. (1) - (11). **Figure 2.1** is the plot of the number of degree distribution versus as a function of cell width, and the line has a slope of -1.35. **Figure 2.2** shows the characteristic path length that the two slopes for our data and random network approaches to -0.42 as the cell width goes to 100km. As shown in **Figure 2.3**, the mean clustering coefficient for our data and random network are increased as the cell width is increased, and the value of mean clustering coefficient for our data approaches to 0.07. The small-worldness value for our data is decreased as the cell width is increased in **Figure 2.4**. The slope of cost efficiency for our data has +1.75 as the cell width goes to 100km in **Figure 2.5**. As shown in **Figure 2.6**, the slope of global efficiency for our data and random network has the same value of +0.28 in the cases of the cell width larger than 30km. **Figure 2.7** is the plot of the modularity Q as a function of cell width, and the functional form of empirical data and random network has the similar linear decay. **Figure 2.8** is the plot of the assortativity r, and the assortativity for empirical data has its values between -0.1 and -0.5, while that for random network approaches to zero. This means that the seismic network of California is anti-assortative with its mere statistical significance.

3. GEOLOGICAL SYSTEM: Seismic Network of Japan

To discuss the earthquake networks based on the seismic data taken in Japan, the data source is the Japan Meteorological Agency (http://www.jma.go.jp/jma/indexe.html). The time interval is between the 5th of March 2003 and the 31th of December 2012. The region covered is 17.95°N-49.30°N latitude and 120.05°W-156.05°W longitude to the depth of 671km. Because we exclude artificial quarry blasts from the data, the data for the total numbers of events is 1,471,803 and contains only events with a magnitude larger than zero.

We summarize the statistical quantities performed from the seismic network of Japan at the five cell widths regions between 5km and 80km in **Table 3.1**, and both our data's network and a random network can be in fact compared and analyzed.

Table 3.1: Numerical computation of statistical quantities performed from seismic time series data taken in Japan. Here, L_{ran} , C_{ran}, E_{ran} , Q_{ran} , and r_{ran}denote the characteristic path length, mean clustering coefficient, global efficiency, modularity, and assortative coefficient of a random network, respectively, and N denotes a number of nodes. Here, we treat these statistical quantities at the five cell widths (5km, 10km, 20km, 40km, and 80km).

cell width (km)	N	C_e	$<k>$	L	L_{rand}	C	C_{rand}	S_w	E	E_{rand}	r	r_{rand}	Q	Q_{rand}
5	216,357	5.38E-05	11.64	3.62	5.28	0.083	5.59E-05	2171.99	0.285	0.193	-0.081	-7.16E-04	0.280	0.253
10	82,831	3.21E-04	26.58	3.10	3.79	0.201	3.28E-04	746.37	0.333	0.269	-0.144	2.01E-04	0.160	0.167
20	24,904	0.0025	62.61	2.72	2.85	0.461	0.0025	191.39	0.382	0.359	-0.240	-8.03E-05	0.089	0.113
40	6,624	0.0167	110.61	2.42	2.14	0.751	0.0167	39.71	0.435	0.483	-0.376	-1.56E-03	0.066	0.085
80	1,663	0.0606	100.80	2.15	1.94	0.879	0.0608	13.08	0.495	0.530	-0.502	2.18E-03	0.091	0.084

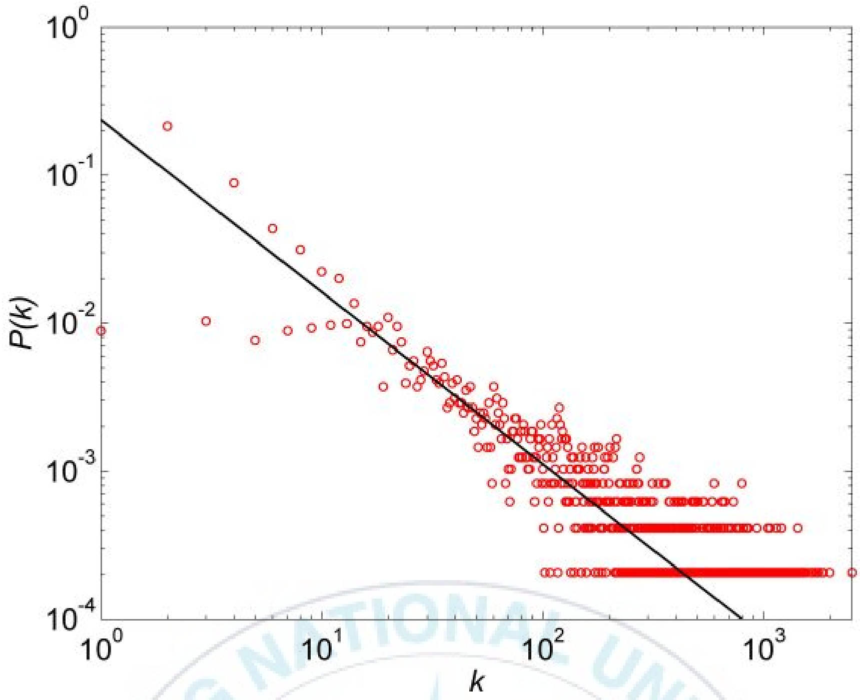

Fig. 3.1: Degree distribution as a function of degree k. The distribution follows a power-law with the scaling exponent -1.16.

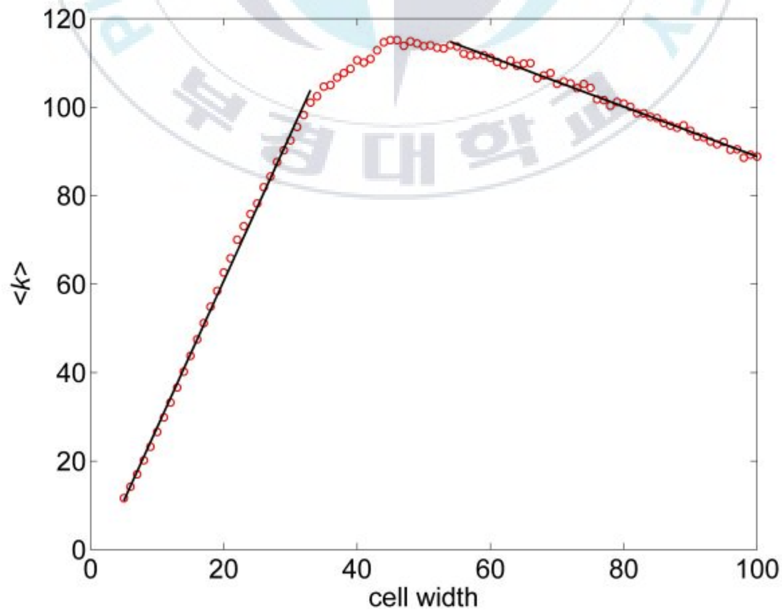

Fig. 3.2: Plot of the mean degree as a function of cell width, where the slope (black line) is +3.31 (-0.56) in the cell width smaller (larger) than 33 (54) km.

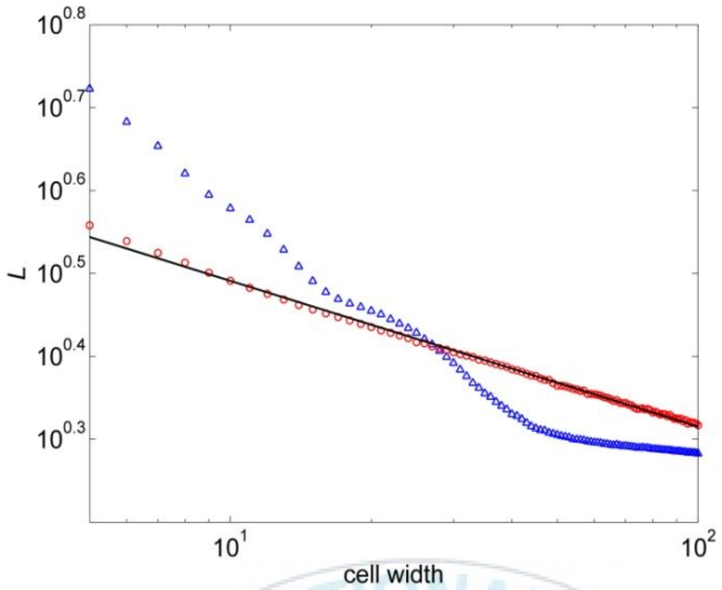

Fig. 3.3: Characteristic path length versus as a function of cell width, where the circle denotes our data and the triangle the random network, and the slope (black line) is -0.18.

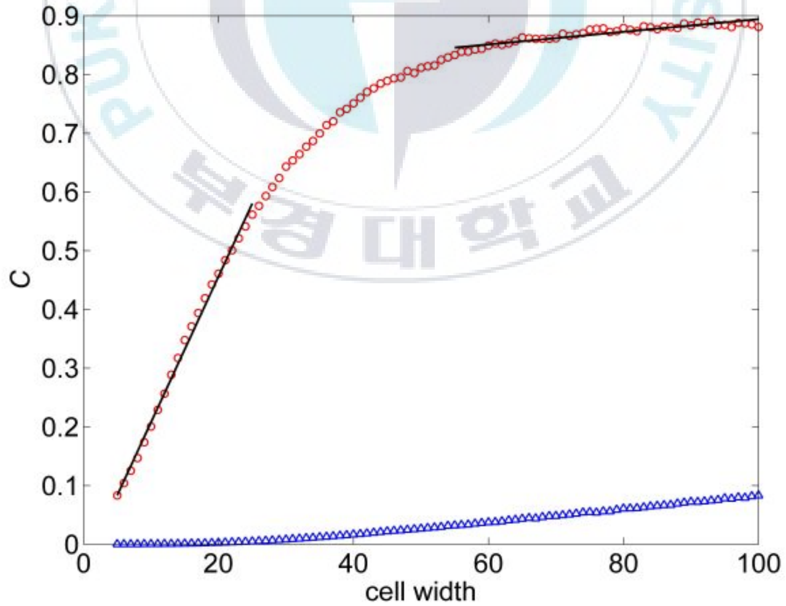

Fig. 3.4: Mean clustering coefficient as a function of cell width, where the circle denotes our data and the triangle the random network. The slope is 0.025 for the cell width smaller than 25km, and the slope is 0.001 for that larger than 55km. The phase transition appears between 25km and 55km.

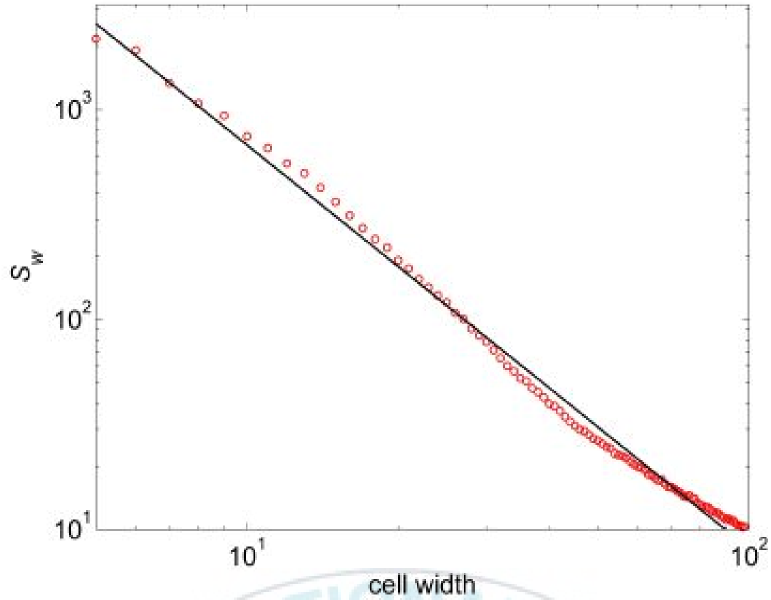

Fig. 3.5: Small-worldness as a function of cell width for our data, and the slope (black line) is -1.92.

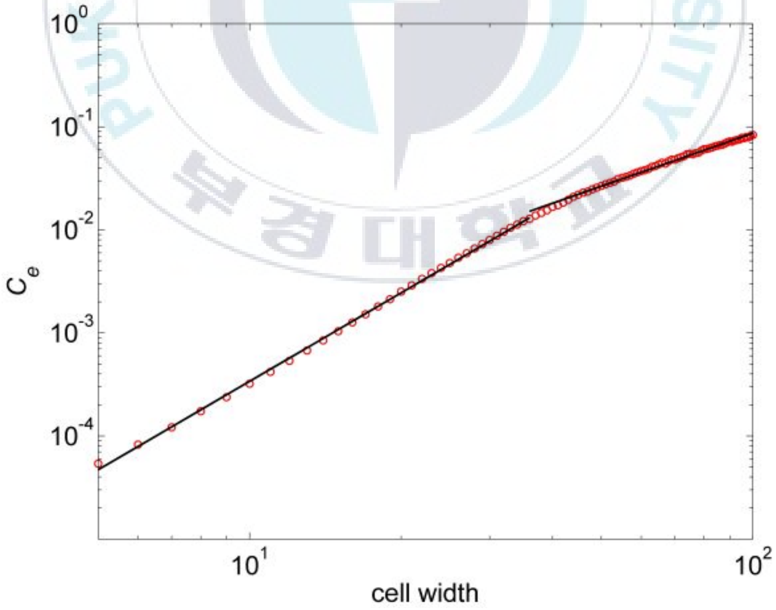

Fig. 3.6: Cost efficiency as a function of cell width. The slope for our data have 2.87 (1.25) for cell widths smaller (larger) than 28 km. Here, we have a phase transition at cell width 28 km.

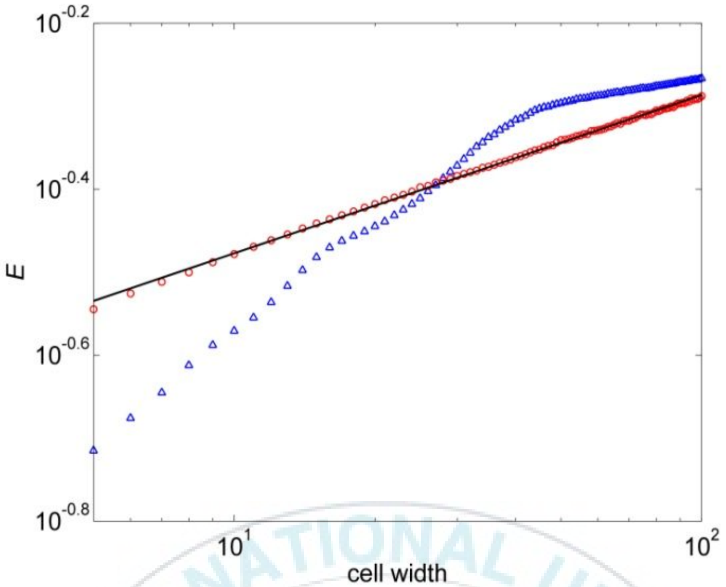

Fig. 3.7: Global efficiency as a function of cell width, where the circle denotes our data and the triangle the random network, where the slope (black line) is 0.19.

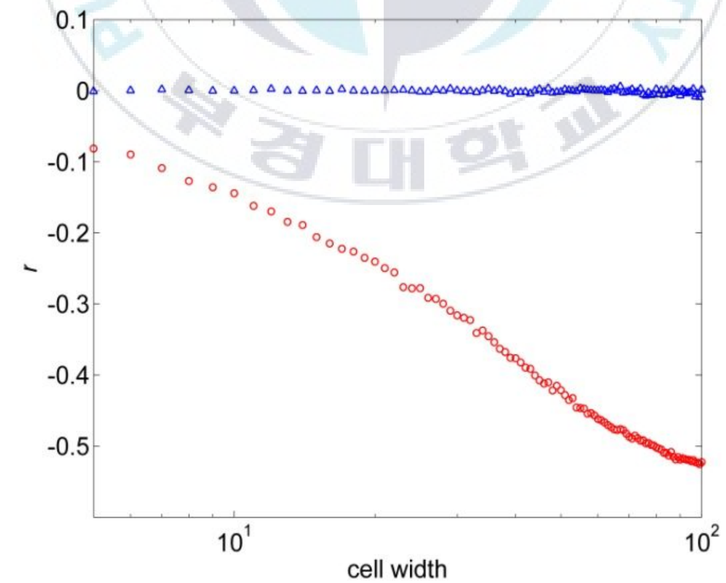

Fig. 3.8: Plot of the assortativity as a function of cell width, where the circle denotes our data and the triangle the random network.

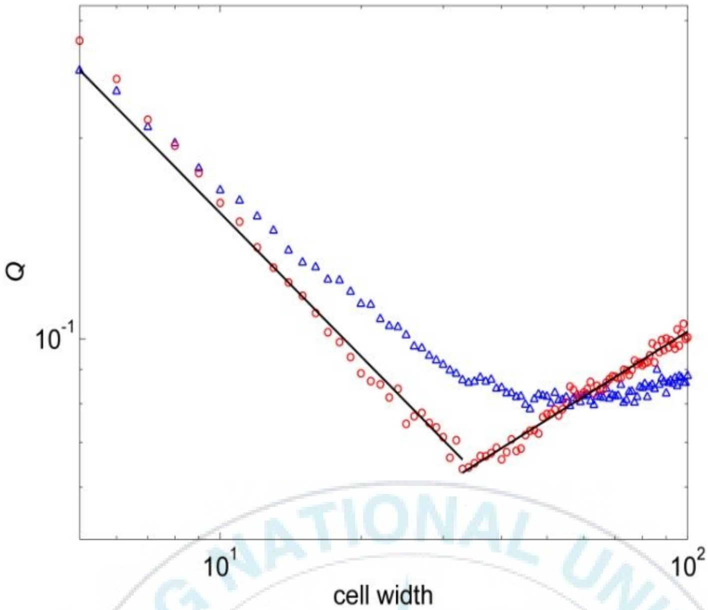

Fig. 3.9: Modularity as a function of cell width, and the circle denotes our data and the triangle the random network. Here we have a phase transition at cell width 33 km, and the slope has -0.71 (0.44) for cell widths smaller (larger) than 125km.

We typically perform the numerical computations for eight statistical quantities given by Eqs. (1) - (11). **Figure 3.1** is the plot of degree distribution having the scale-free network as a function of cell width, and the line has a slope of -1.16. **Figure 3.2** plots the mean degree as a function of cell width. The slope is +3.31 in the cell width smaller than 33km, and the slope is -0.56 in the cell width larger than 54km.

Figure 3.3 shows the characteristic path length that the two slopes for our data and random network approaches to -0.39 as the cell width goes to 100km. As shown in **Figure 3.4**, the mean clustering coefficient has almost linear slope for the cell widths smaller than 25km and larger than 55km. It may be inferred that there exists one phase transition for the cell widths between 25km and 55km.

The small-worldness value for our data is decreased as the cell width is increased in **Figure 3.5**, and its slope has -1.92 as the cell width goes to 10^2 *km*. The values decrease monotonously from 2,272 to 9.97. Since the values are much larger than 1, it satisfies the small-worldness property. In **Figure 3.6**, there is one phase transition for the cost efficiency at cell width 28km approximately. The slopes for our data have 2.87 for cell widths smaller than 28km and 1.25 for cell widths larger than 28km, respectively. As shown in **Figure 3.7**, the slope of the global efficiency for our data has 0.19, not similar to the random controls.

Figure 3.8 is the plot of the assortativity r as a function of cell width, and the modularity has its values between -0.082 and -0.502, while that for random network approaches to zero. Since the values for the assortativity are smaller than zero, we suggest that the seismic network of Japan is not assortative, i.e., the rich nodes have a tendency to be connected to the poors. **Figure 3.9** is the plot of the modularity Q as a function of cell width, and we particularly have a phase transition at cell width 33km, similar to the cost efficiency.

4. ECONOMIC SYSTEM: Visibility Network of Korea Stock Market

To discuss economic networks based on financial data, we use the KOSPI and KOSDAQ of the Korean financial market. We extract the price of all stocks from the KOSPI and KOSDAQ that were exchanged on the Korean stock market during a period 1996 – 2014. We typically perform the numerical computations for the global efficiency, the assortative coefficient, and the modularity given by Eqs. (7), (10), and (11).

Table 4.1 summarizes the values of eight statistical quantities for the KOSPI and KOSDAQ.

Table 4.1: Numerical computation of statistical quantities performed from (a) the KOSPI and (b) the KOSDAQ. Here, the L, C_g, $C_{g,\,rand}$, S_w, E_g, $E_{g,\,rand}$, Q, Q_{rand}, r and r_{rand} denote, the average values of the characteristic path length, global clustering coefficient, small-worldness, global efficiency, modularity, and assortativity in financial networks, and their random control, respectively.

(a) KOSPI

N	$<k>$	Slope of degree distribution	L	L_{rand}	C_g	$C_{g,\,rand}$	S_w	E_g	$E_{g,\,rand}$	Q	Q_{rand}	r	r_{rand}
1000	20.238	-1.337	3.770	2.632	0.657	0.021	22.056	0.301	0.401	0.560	0.203	0.227	-0.007
1500	18.816	-1.458	4.292	2.790	0.666	0.012	34.805	0.264	0.374	0.657	0.217	0.252	0.001
2000	19.343	-1.536	4.467	2.851	0.663	0.009	43.312	0.252	0.365	0.723	0.211	0.226	0.004
2500	21.458	-1.483	4.353	2.846	0.657	0.008	49.082	0.256	0.364	0.671	0.202	0.212	-0.003
3000	22.844	-1.486	4.355	2.854	0.657	0.007	58.276	0.259	0.362	0.655	0.192	0.195	-0.003
3500	22.480	-1.551	4.657	2.904	0.653	0.006	65.003	0.242	0.355	0.680	0.193	0.218	-0.002
4000	22.171	-1.592	4.894	2.952	0.655	0.005	72.954	0.231	0.349	0.725	0.192	0.209	-0.006
4500	20.850	-1.645	5.261	3.043	0.662	0.004	84.821	0.217	0.339	0.744	0.190	0.240	-0.015
4650	20.502	-1.656	5.301	3.072	0.664	0.004	88.321	0.214	0.336	0.741	0.194	0.247	0.003

(b) KOSDAQ

N	$<k>$	Slope of degree distribution	L	L_{rand}	C_g	$C_{g,\,rand}$	S_w	E_g	$E_{g,\,rand}$	Q	Q_{rand}	r	r_{rand}
1000	29.478	-1.124	3.461	2.377	0.617	0.029	14.164	0.343	0.446	0.429	0.163	-0.180	0.005
1500	29.034	-1.249	3.819	2.539	0.617	0.018	21.981	0.304	0.416	0.601	0.164	-0.171	0.004
2000	28.429	-1.337	3.902	2.643	0.624	0.014	29.514	0.294	0.397	0.621	0.171	-0.196	-0.007
2500	34.590	-1.302	3.830	2.597	0.607	0.013	29.517	0.299	0.405	0.557	0.153	-0.188	0.005
3000	33.918	-1.336	3.900	2.662	0.611	0.011	36.325	0.292	0.393	0.581	0.156	-0.172	-0.006
3500	32.689	-1.397	3.994	2.720	0.613	0.009	44.325	0.283	0.382	0.615	0.160	-0.145	0.004
4000	31.971	-1.410	3.983	2.761	0.616	0.007	54.325	0.282	0.375	0.609	0.162	-0.144	0.001
4500	31.785	-1.416	3.974	2.788	0.617	0.006	62.197	0.281	0.371	0.607	0.162	-0.143	-0.001
4650	31.660	-1.421	3.993	2.796	0.618	0.006	63.768	0.280	0.369	0.605	0.164	-0.145	0.005

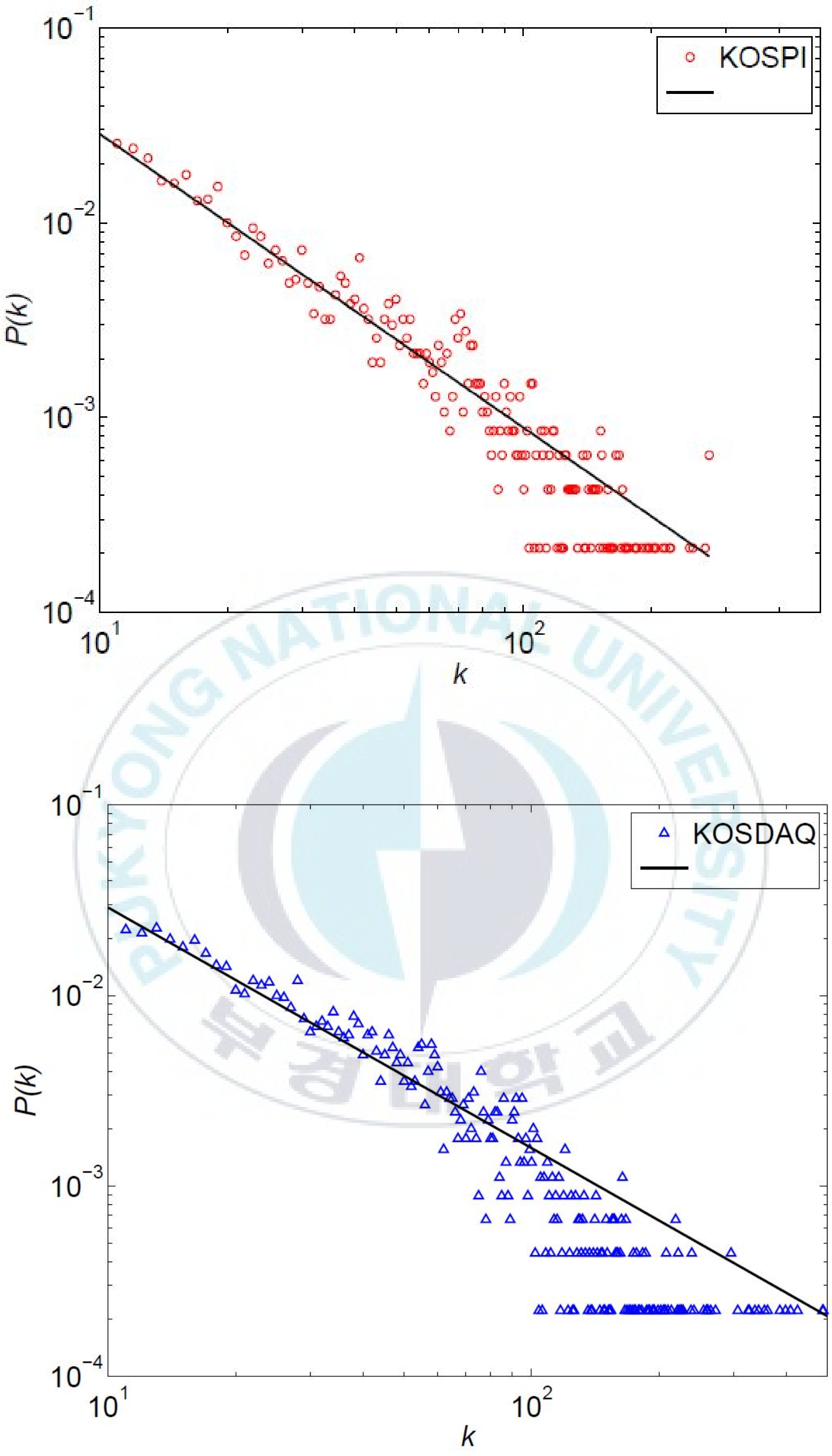

Fig. 4.1: Degree distribution of the KOSPI data (top) and the triangle the KOSDAQ data (down) versus as a function of k. The distributions follow a power-law with the scaling exponents -1.656 and -1.421.

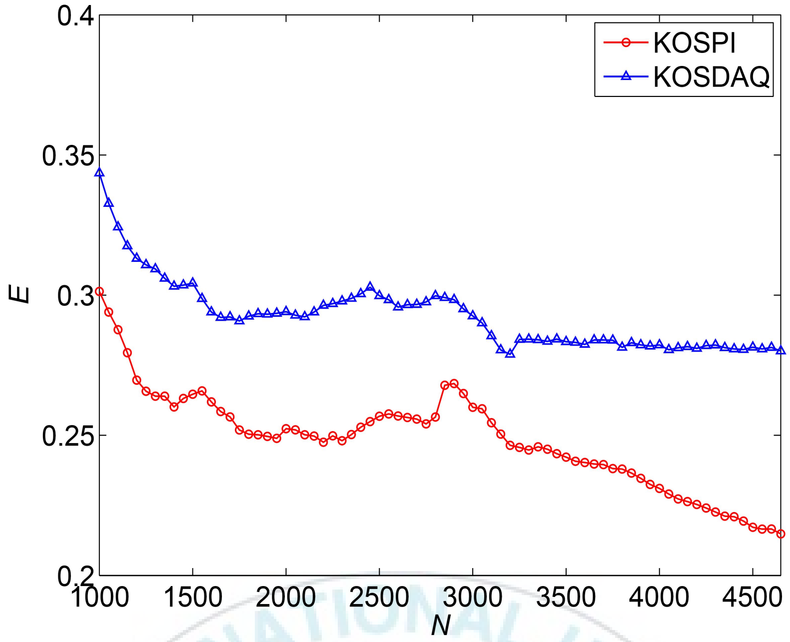

Fig. 4.2: Global efficiency as a function of the node, where the circle denotes the KOSPI data and the triangle the KOSDAQ data.

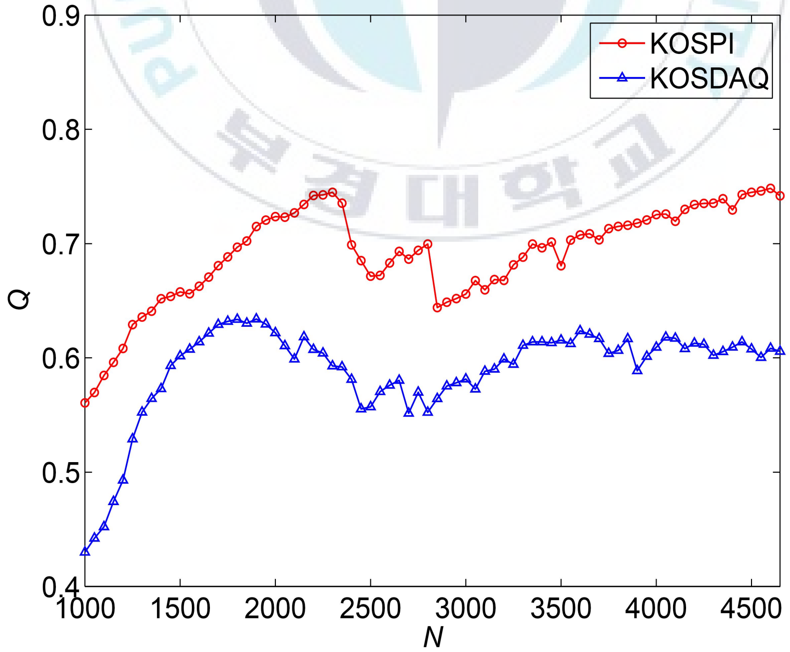

Fig. 4.3: Modularity as a function of the node, where the circle denotes the KOSPI data and the triangle the KOSDAQ data.

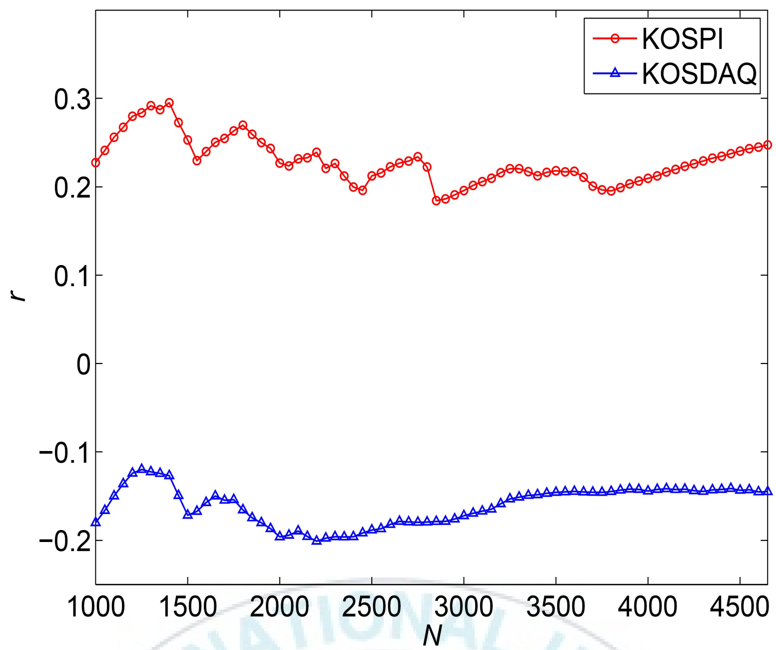

Fig. 4.4: Assortative coefficient as a function of the node, where the circle denotes the KOSPI data and the triangle the KOSDAQ data.

Figure 4.1 is a plot of degree distribution of the KOSPI and the KOSDAQ. The degree distribution of the KOSPI shows a power law with the scaling exponent -1.656 while that of the KOSDAQ shows a power law with the scaling exponent -1.421. These are the slopes of the degree distribution when the node is $N=4,650$. In **Figure 4.2**, we show the global efficiency of the KOSPI and the KOSDAQ. The value of the KOSPI decreases monotonously from 0.301 to 0.214 while the value of the KOSDAQ decreases monotonously from 0.343 to 0.280. **Figure 4.3** is a plot of the modularity as a function of the node. The value of the KOSPI increases monotonously from 0.195 to 0.247 while the value of the KOSDAQ increases monotonously from 0.560 to 0.744. In **Figure 4.4**, we show the plot of the assortative coefficient of the KOSPI and the KOSDAQ as a function of the node. Similar to the modularity, the value of the KOSPI increases monotonously from 0.195 to 0.247 while the value of the KOSDAQ increases monotonously from -0.180 to -0.143. Hence, we show that the KOSPI is more assortative than the KOSDAQ.

5. SOCIAL SYSTEM: Communicability Network for Authors of Korean Meteorological Society

We deal with the 2,508 proceeding papers and 1,943 authors (these are the nodes of the network) in conferences of the Korean meteorological society from March 2008 and November 2013.

We implement the computer-simulation of the four communicability functions from Eqs. (14), (15), (22), and (26).

Table 5.1: Values of the averaged communicability functions and the weight of community (W_C), where these are normalized values divided by the maximum value of each factors for the 200-th, 400-th, ..., and 1,800-th authors, respectively.

Sequent order of author	W_C	G_p^{EA}	G_p^{RA}	G_p^{EL}	$1/G_p^{D}$
200	0.0374	0.085	0.070	0.997	0.115
400	0.098	0.001	0.030	0.967	0.055
600	0.017	0.005	0.020	0.925	0.037
800	0.018	0.007	0.015	0.838	0.016
1000	0.010	0.002	0.010	0.757	0.021
1200	0.031	0.002	0.008	0.612	0.014
1400	0.006	0.001	0.005	0.518	0.011
1600	0.006	0	0.004	0.451	0.006
1800	0.003	0	0.004	0.423	0.008

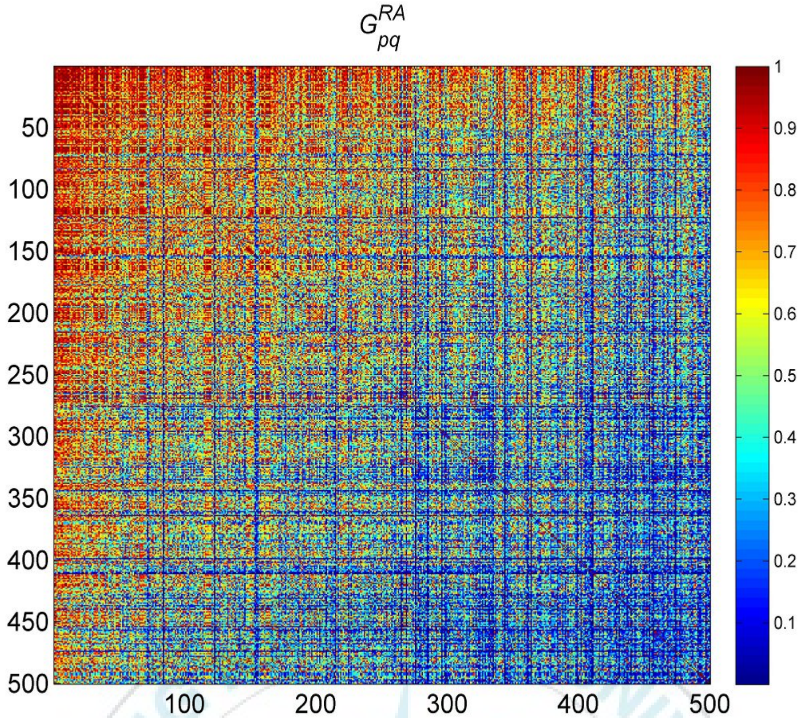

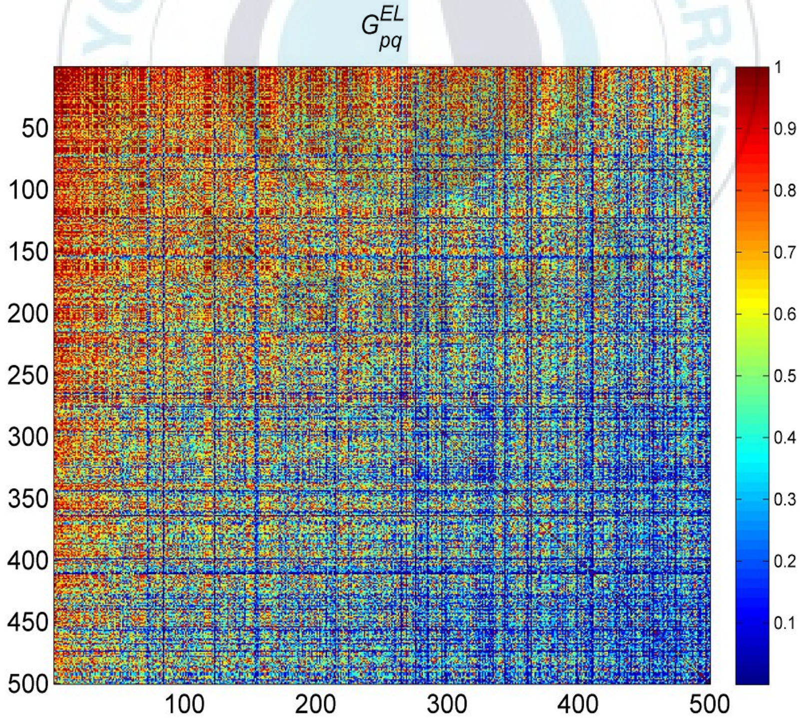

Fig. 5.1: Color map diagram of relative communicability function matrices G_{pq}^{RA} (top) and G_{pq}^{EL} (down) for major 500 members of the author network.

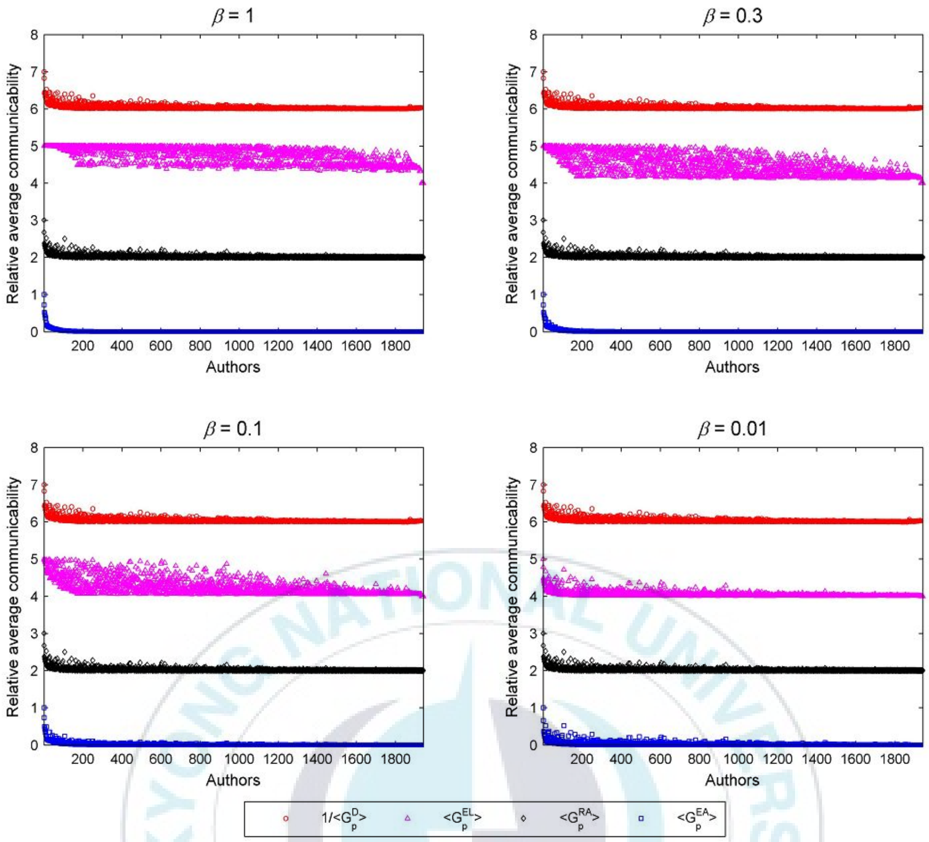

Fig. 5.2: Values of averaged communicability functions, G_p^{EA}, G_p^{RA}, G_p^{EL}, and $1/G_p^D$ for four beta values. Here, note that G_p^D increases as the other indices decrease.

Table 5.1 summarizes the values of the averaged communicability functions and the weight of community for 200-th, 400-th, ..., and 1,800-th authors, respectively. These values are normalized values divided by the maximum value of each factors. The value of G_p^{EA} for two authors, 1,600-th, and 1,800-th authors, approaches to zero. We find that the G_p^{EL} have relatively hight values compared to the other communicabilities for each author.

Figure 5.1 shows the color-map diagram of the communicability function matrices G_{pq}^{RA} and G_{pq}^{EL} for major 500 members of 1,943 authors for the Korean meteorological society publications, among four communicability functions [25]. If two members are highly correlated, the representation approaches the color red. If they are weakly correlated, the representation approaches dark blue.

From Eq. (28), we can simulate four averaged communicability functions. **Figure 5.2** is the plot of the averaged communicability functions for 1,943 members of the author network for four beta values. We assume that the weight of the community for the primary author is twice of the other authors. For instance, if a paper is made by n authors, then the weight of the primary author is $2n/[(n-1)(n+2)]$ and that of the other authors are $n/[(n-1)(n+2)]$. Then, sum of all weight of community is exactly n for the paper. We treat the values of the averaged communicability functions such as the G_p^{EA}, G_p^{RA}, G_p^{EL}, and $1/G_p^D$. It is actually known that the G_p^D increases as the other functions decrease, and here we calculate $1/G_p^D$ instead. We now speculate that the phase transition among these functions may exist near the 200-th authors. Next time, we aim to find it through networks of other societies.

IV. CONCLUSION

Complex network theory is developed dramatically in past decades. The main concern is translated to the non-equilibrium, dynamics, evolution, etc. We have studied the dynamics of network properties with several statistical quantities in some scientific phenomena.

First, we have studied the protein contact network of amino acid in biological system. General measures of network, i.e., characteristic path length, clustering coefficient, efficiency, modularity, and assortativity, reflected the topological characteristics of biological networks, different from the random controls in biological structures. We examined introduce four major protein groups (α, β, $\alpha+\beta$, and α/β) enumerated in the Structural Classification of Proteins to characterize the networks in this work. Our results showed that protein structures have small-world networks regardless of their structural classification across four major groups [111]. Particularly, the average values for the distribution of local and global clustering coefficients are, respectively, 0.554±0.028 and 0.503±0.023 in the protein networks. The average degrees of the α, β, $\alpha+\beta$, and α/β groups are calculated to have similar values near 10. The specific restrictions are responsible for the emergence of different classes of networks with characteristic degree distributions [112]. It was observed that the preferential attachment to vertices in many real scale-free networks can be hindered by factors like ageing of the vertices (e.g. actor networks) [113,114], cost of adding links to the vertices, or the limited capacity of a vertex (e.g. airports network) [115,116]. Specifically the averaged local and global clustering coefficients have values near 0.5 in the protein networks, while the random controls have the same values as 0.036. The averaged value of modularity for the four protein groups is larger than that of the random controls. We also found that averaged value for global efficiency smaller than that of random controls, while the averaged value of local efficiency is larger than that of random controls. It has been recognized that the results obtained from biological networks were related to the small-world or scale-free networks between degrees, but we found that the small-world structure existed in protein networks. Our findings support the idea that the recent network approaches to biological networks is very reliable. In the future, the formalism of our analysis will be useful as it can be extended to both the discrimination and the characterization of various bio-networks.

Second, we have examined the topological properties of the earthquake network in geological system by using the seismic data from southern California in the USA. Our estimated metrics were found by using network theory, and we ascertained that there is no hierarchy structure in the seismic network. In present, our result is one trial for several statistical quantities of the seismic network unstudied. The universal and irregular properties of seismic network are not found, but it may be in future anticipated to deduce these properties as many researchers simulate and analyze several methods and high techniques in scientific fields of seismic networks [117-119], different from the small-world network and the scale-free network. We believe that the idea by which this result is obtained may be a useful starting point for a new approach to understanding the topological properties of network theory in the seismology. Our findings support the finding that a recent network approach to seismic analysis is very reliable in three-dimensional cells. Our hope is that our analysis will be extended to both the discrimination and the characterization of various earthquakes in other nations.

Third, we have treated the seismic network in geological system by considering the volume resolution and the temporal causality. We have examined the topological properties of the earthquake network by using the seismic data from Japan. Our estimated metrics are found by using the network theory, and we ascertain that there is no hierarchy structure in the seismic network. Furthermore, the statistical quantities in network theory turn out that these scaling exponents have not invariant or universal properties as yet from our result. In present, our result is one trial for several statistical quantities of the Japanese seismic network studied and analyzed, and we particularly have a phase transition for the cost efficiency and the modularity. Interestingly, the mean clustering coefficient tends to increase as the cell width goes to $100\mathrm{km}$. We had the values between 0.85 and 0.90 in the cell-widths between $60\mathrm{km}$ and $100\mathrm{km}$ for our data, while Abe and Suzuki [120] amazingly discovered the universal $C \sim 0.85$ scaling with respect to dimensionless cell-size in the three-dimensional networks of California and Japan. The universal and irregular properties of seismic network are not found as yet from our data, but it may be in future anticipated to deduce these properties as many researchers simulate and analyze several methods and high techniques in scientific fields of seismic networks [117,119-121], different from the small-world network and the scale-free network. We believe that the general idea by which this result is obtained may be the point of a subject for a new approach to understanding and developing the topological properties of network theory in the seismology field. Our findings supports that a recent network approach to seismic analysis is very useful and reliable in three-dimensional cells. It is anticipated that our analysis will be extended to both the discrimination and the characterization of various earthquakes in other Continents.

Forth, we investigate the network metrics in a time series of the KOSPI and the KOSDAQ indices converting by the visibility algorithm as an economic system. The KOSPI and the KOSDAQ by adopting the visibility algorithm is proportional to a power law rather than the Poisson distribution. We mainly simulate and analyze the network metrics from the nodes and its links in the financial networks. The increases of the assortative coefficient and the modularity would particularly be targets comparable to other statistical quantities in future. The universal and irregular properties of statistical quantities in financial network do not find unambiguously, but it may be inferred that these topological properties improve by implementing the statistical method and its technique from registered data of financial networks. We cannot find the statistical quantities behave regularly and phase-transitionally with the node in the visibility algorithm [122,123] of Korean financial markets, but the increases of the assortative coefficient and the modularity would particularly may become attractable targets compared to statistical quantities of other different fields in future. We believe that the general idea by which this result is obtained may be the point of a subject for a new approach to understanding and developing the topological properties of network theory in financial markets. Our findings support that a recent network approach to our analysis is very useful and reliable in financial markets. It is anticipated that our analysis will be extended to both the discrimination and the characterization of various markets in other nations.

Lastly, we have studied the community structure of Korean meteorology fields in the 1,943 author networks of all Korean meteorological society proceedings in conferences from March 2008 to November 2013 as a social system. We mainly implemented the computer-simulation of the four communicability functions. To compare the four averaged communicability functions, it was shown that the G_p^{EL} constructs a stronger community structure rather than the other three. The function G_p^{EA} finds the community structure weaker than the other three as well. We can make use of the four averaged communicability functions to compute the measures of a community structure, and it is hoped that our method and technique will lead us to more general results in the future. It is not trustworthy now, but we anticipate that the phase transition among the averaged communicability functions may exist at one value near 200-th authors. Our results cannot yet be compared to that of other social networks, but we hope to compare to our results to other successful results in social networks that have been prominently produced and published. Next time, we hope to discuss the phase transition of the averaged communicability functions, with network systems of other societies. In the future, we will apply the community structure to the cases of different contributed weight between authors. Therefore, further work is needed for the case with societies of more than the author and citation networks [124-126]. The formalism of our analysis can be extended to both the discrimination and the characterization of communicability functions in other various societies.

REFERENCES

[1] A. Nobi, S. E. Maeng, G. G. Ha and J. W. Lee, J. Korean Phys. Soc. **62**, 569 (2013).

[2] M. W. Cho, J. Korean Phys. Soc. **64**, 1213 (2014).

[3] H. W. Choi, S. E. Maeng and J. W. Lee, J. Korean Phys. Soc. **60**, 657 (2012).

[4] G. Caldarelli, *Scale-Free Networks: Complex Webs in Nature and Technology*, Oxford University Press, Oxford, 2007.

[5] J. Ku, J. W. Ryu, H. Y. Kim and J. S. Yoo, J. Korean Phys. Soc. **60**, 527 (2012).

[6] M. Girvan and M. E. J. Newman, Proc. Nat. Acad. Sci. USA **99**, 7821 (2002).

[7] S. Fortunato, Phys. Rep. **486**, 75 (2010).

[8] S. H. Yook, Z. N. Oltvai and A.-L. Barabasi, Proteomics **4**, 928 (2004) .

[9] H. Jeong, B. Tombor, R. Albert, Z. N. Oltvai and A.-L. Barabashi, Nature **407**, 651 (2000).

[10] E. Ravsaz, A. L. Somera, D. A. Mongru, Z. N. Oltvai and A.-L. Barabashi, Science **297**, 1551 (2002).

[11] R. Albert and H. G. Othmer, J. Theor. Biol. **223**, 1 (2003).

[12] A. Aszodi and W. R. Taylor, CABIOS **9**, 523 (1993).

[13] M. Vendruscolo, N. V. Dokholyan, E. Paci and M. Karplus, Phys. Rev. E **65**, 061910 (2002).

[14] L. H. Greene and V. A. Higman, J. Mol. Biol. **334**, 781 (2003).

[15] A. R. Atilgan, P. Akan and C. Baysal, Biophys. J. **86**, 85 (2004).

[16] A.-L. Barabashi and Z. N. Oltvari, Nat. Rev. Genet. **5**, 101 (2004).

[17] L. Giot et al., Science **302**, 1727 (2003).

[18] H. Jeong, S. P. Mason, A.-L. Barabashi and Z. N. Oltvai, Nature **411**, 41 (2001).

[19] S. Li et al., Science **301**, 540 (2004).

[20] A. Wagner, Mol. Biol. and Evol. **18**, 1283 (2001).

[21] A. G. Murzin, S. E. Brenner, T. Hubbard and C. Chothia, J. Mol. Biol. **247**, 536 (1995).

[22] Y. Kim, New Physics **64**, 1 (2014).

[23] T. C. Halsey, M. H. Jensen, L. P. Kanadanoff, I. Procaccia and B. I. Shraiman, Phys. Rev. B **33**, 1141 (1986).

[24] J. L. McCauley, Phys. Rep. **189**, 225 (1990).

[25] B. B. Mandelbrot, J. Fluid Mech. **62**, 331 (1974).

[26] R. Liu, T. D. Matteo and T. Lux, Fractals **11**, 669 (2008).

[27] G. Lim, S.-Y. Kim, H. Lee, K. Kim and D.-I. Lee, Physica A **386**, 259 (2007).
[28] M. Gallegati, A. Palestrini and M. Petrini, Fractals **11**, 119 (2008).
[29] S. M. Debbal and F. Bereksi-Reguig, Fractals **19**, 331 (2007).
[30] K-I. Goh, E. Oh, H. Jeong, B. Kahng and D. Kim, Proc. Nat. Acad. Sci. **99**, 12583 (2002).
[31] C. Song, S. Havlin and H. A. Makse, Nature **433**, 392 (2005).
[32] S. Abe and N. Suzuki, Nonlin. Proc. Geophys. **13**, 145 (2006).
[33] D-H. Kim and H. Jeong, Phys. Rev. E **72**, 046133 (2005).
[34] S-H. Yook, J. Korean, Phys. Soc. **56**, 990 (2010).
[35] J. Kong, J. Korean Phys. Soc. **55**, 2248 (2009).
[36] H-D. J. Jeong, J. Korean, Phys. Soc. **55**, 2072 (2009).
[37] S. Abe and N. Suzuki, Physica A **388**, 2511 (2009).
[38] L. Telesca, V. Lapenna and M. Macchiato, Physica A **354**, 629 (2009).
[39] F. Omori, J. Coll. Sci. Imp. U. Tok. **7**, 111 (1894).
[40] T. Utsu, Geophys. Mag. **30**, 521 (1961).
[41] S. Boccaletti, V. Latora, Y. Moreno, M. Chavez and D. U. Hwang, Phys. Rep. **424**, 175 (2006).
[42] S. A. Jung, J. H. Jung, D. I. Lee, J.W. Jung, K. H. Chang, D. H. Ha, S. Y. Kim and K. Kim, J. Korean Phys. Soc. **56**, 1877 (2010).
[43] S. Abe and N. Suzuki, J. Geophys. Res. **108**, 2113 (2003).
[44] S. Abe and N. Suzuki, Physica A **319**, 522 (2003).
[45] C. Tsallis, J. Stat. Phys. **52**, 479 (1988).
[46] S. Abe and N. Suzuki, Physica A **332**, 533 (2004).
[47] S. Abe and N. Suzuki, Europhys. Lett. **65**, 581 (2004).
[48] J. P. Wang, X. Yun and S. C. Chang, Physica A **413**, 385 (2014).
[49] X. He, H. Zhao, W. Cai, Z. Liu and S.-Z. Si, Physica A **413**, 175 (2014).
[50] S. Boccaletti, G. Bianconi, R. Criado, C. I. del Genio, J. Gómez-Gardeñes, M. Romance, I. Sendiña-Nadal, Z. Wang and M. Zanin, Phys. Rep. **544**, 1 (2014).
[51] Y. S. Cho, S. Hwang, H. J. Herrmann and B. Kahng, Science **339**, 1185 (2013).
[52] S. Min and K. Kim, J. Korean Phys. Soc. **65**, 946 (2014).
[53] W. H. Baek, G. Lim, K. Kim, Y.-J. Choi, K.-H. Chang, J.-W. Jung, M. Yi, D.-I. Lee and D.-H. Ha, Physica A **391**, 2279 (2012).

[54] T. P. Peixoto and C. P. C. Prado, Phys. Rev. E **69**, 025101 (2004).

[55] T. P. Peixoto and C. P. C. Prado, e-print condmat/0602244, (2006).

[56] A. Nobi, S. E. Maeng, G. G. Ha and J. W. Lee, J. Korean Phys. Soc. **66**, L1153 (2015).

[57] G. Oh, J. Korean Phys. Soc. **64**, 1751 (2014).

[58] Y. S. Cho, S. Hwang, H. J. Herrmann, and B. Kahng, Science **339**, 1185 (2013).

[59] F. Schweitzer, G. Fagiolo, D. Sornette, F. Vega-Redondo, A. Vespignani and D. R.White, Science **325**, 422 (2009).

[60] L. Laloux, P. Cizeau, J.-P. Bouchaud and M. Potters, Phys. Rev. Lett. **83**, 1467 (1999).

[61] V. Plerou, P. Gopikrishnan, B. Rosenow, L. A. N. Amaral and H. E. Stanley, Phys. Rev. Lett. **83**, 1471 (1999).

[62] V. Plerou, P. Gopikrishnan, B. Rosenow, L. A. N. Amaral, T. Guhr and H. E. Stanley, Phys. Rev. E **65**, 066126 (2002).

[63] R. N. Mantegna, Eur. Phys. J. B **11**, 193 (1999).

[64] J.-P. Onnela, A. Chakraborti, K. Kaska and J. Kertesz, Physica A **324**, 247 (2003).

[65] J. Zhang and M. Small, Phys. Rev. Lett. **96**, 238701 (2006).

[66] J. Zhang, J.-F. Sun, X.-D. Luo, K. Zhang, T. Nakamura and M. Small, Physica D **237**, 2856 (2008).

[67] Y. Yang and H.-J. Yang, Physica A **387**, 1381 (2008).

[68] Z.-K. Gao and N.-D. Jin, Phys. Rev. E **79**, 066303 (2009).

[69] X.-K. Xu, J. Zhang and M. Small, Proc. Natl. Acad. Sci. U.S.A. **105**, 19601 (2008).

[70] P. Li and B.-H. Wang, Chinese Science Bulletin **51**, 624 (2006).

[71] P. Li and B.-H. Wang, Physica A **378**, 519 (2007).

[72] L. Lacasa, B. Luque, F. Ballesteros, J. Luque and J. C. Nuno, Proc. Natl. Acad. Sci. U.S.A. **105**, 4972 (2008).

[73] C.-B. Li, H. Yang and T. Komatsuzaki, Proc. Natl. Acad. Sci. U.S.A. **105**, 536 (2008).

[74] A. H. Shirazi, G. R. Jafari, J. Davoudi, J. Peinke, M. R. R. Tabar and M. Sahimi, J. Stat. Mech. P07046 (2009).

[75] X.-H. Ni, Z.-Q. Jiang and W.-X. Zhou, Phys. Lett. A **373**, 3822 (2009).

[76] L. Lacasa, B. Luque, J. Luque and J. C. Nuno, Europhys. Lett. **86**, 30001 (2009).

[77] J. B. Elsner, T. H. Jagger and E. A. Fogarty, Geophys. Res. Lett. **36**, L16702 (2009).

[78] Y. Yang, J.-B. Wang, H.-J. Yang and J.-S. Mang, Physica A **388**, 4431 (2009).

[79] Y. Kim, W. Choi and S.-H. Yook, J. Korean Phys. Soc. **60**, 621 (2012).

[80] E. Estrada, N. Hatano and M. Benzi, Phys. Rep. **514**, 89 (2012).

[81] E. Estrada and N. Hatano, Phys. Rev. E **77**, 036111 (2008).

[82] L. da Fontoura Costa, O. N. Oliveira Jr., G. Travieso, F. A. Rodrigues, P. R. Villas Boas, L. Antiqueira, M. P. Viana and L. E. Correa Rocha, Adv. Phys. **60**, 329 (2011).

[83] M. E. J. Newman, SIAM Rev. **45**, 167 (2003).

[84] M. J. E. Newman, *Networks*, Oxford University Press, Oxford, 2010.

[85] S. H. Strogatz, Nature 419, **268** (2001).

[86] D. J. Watts, *Small Worlds: The Dynamics of Networks Between Order and Randomness*, Princeton University Press, Princeton, 2003.

[87] M. Buchanan, *The Social Atom*, Cyan Books and Marshall Cavendish, 2007.

[88] R. N. Mantegna and E. H. Stanley, *Introduction to Econophysics: Correlations and Complexity in Finance*, Cambridge University Press, Cambridge, 1999.

[89] B. K. Chakrabarti, A. Chakraborti and A. Chatterjee, *Econophysics and Sociophysics: Trends and Perspectives*, Wiley VCH, Berlin, 2006.

[90] J. A. Dunne, R. J. Williams and N. D. Martinez, Ecol. Lett. **5**, 558 (2002).

[91] F. Jordan and I. Scheuring, Oikos **99**, 607 (2002).

[92] E. Zotenko, J. Mestre, D. P. O'Leary and T. M. Przytycka, PLoS Comput. Biol. **4**, e1000140 (2008).

[93] J. Y. Kim and K.-I. Goh, Phys. Rev. Lett. **111**, 058702 (2013).

[94] A.-L. Barabasi and R. Albert, Science **286**, 509 (1999).

[95] V. Latora and M. Marchiori, Phys. Rev. Lett. **87**, 198701 (2001).

[96] M. E. J. Newman, Phys. Rev. Lett. **89**, 208701 (2002).

[97] M. E. J. Newman, Proc. Natl. Acad. Sci. USA **103**, 8577 (2006).

[98] S. Min and K. Kim, unpublished.

[99] D. Cvetković, P. Rowlinson and S. Simić, *Eigenspaces of Graphs*, Cambridge University Press, Cambridge, 1997.

[100] F. Harary and A. J. Schwenk, Pacific J. Math. **80**, 443 (1979).

[101] E. Estrada and J. A. Rodriguez-Velazquez, Phys. Rev. E **71**, 056103 (2005).

[102] N. Higham, *Function of Matrices*, Philadelphia, PA, (2008).

[103] L. C. Freeman, Social Netw. **1**, 215 (1979).

[104] S. Wasserman and K. Faust, *Social Network Analysis*, Cambridge University Press, Cambridge, 1994.

[105] E. Estrada and N. Hatano, Physica A **389**, 3648 (2010).

[106] E. Estrada and N. Hatano, Chem. Phys. Lett. **486**, 166 (2010).
[107] H. M. Berman, J. Westbrook, Z. Feng, G. Gilliland, T. N. Bhat, H. Weissig, I. N. Shindyalov, P. E. Bourneand and W. R. Taylor, Nucleic Acids Res. **28**, 235 (2000).
[108] R. Albert and A.-L. Barabashi, Rev. Mod. Phys. **74**, 47 (2002).
[109] W. H. Press, S. A. Teukolsky, W. T. Vetterling and B. P. Flannery, *Numerical Recipes in C*, 2nd Edition, Cambridge University Press, 1993.
[110] S. Min and K. Kim, unpublished.
[111] G. Bagler and S. Sinha, Physica A **346**, 27 (2005)
[112] L. A. N. Amaral, A. Scala, M. Barthelemy and H. E. Stanley, Proc. Natl. Acad. Sci. **97**, 11149 (2000).
[113] B. Kahng,_ K.-I. Goh, D.-S. Lee and D. Kim, Sae Mulli **48**, 115 (2004).
[114] D. R. Amancio, N. Osvaldo, Jr. Oliveira and L. F. Costa, Europhys. Lett. **99**, 48002 (2012).
[115] P. Fleurquin, J. J. Ramasco and V. M. Eguiluz, Scien. Rep. **3**, 1159 (2013).
[116] Marko Popovic, Hrvoje Stefancic and Vinko Zlatic, Phys. Rev. Lett. **109**, 208701 (2012).
[117] S. Abe and N. Suzuki, Europhys. Lett. **87**, 48008 (2009).
[118] S. Abe and D. Pasten, N. Suzuki, Physica A **390**, 1343 (2011).
[119] S. Abe and N. Suzuki, Phys. Rev. E **74**, 026113 (2006).
[120] S. Abe and N. Suzuki, Physica A **421**, 343 (2015).
[121] S. Abe, D. Pasten and N. Suzuki, Physica A **390**, 1343 (2011).
[122] A. Snarskii and I. Bezsudnov, arXiv:1302.3265.
[123] M.-C. Qian, Z.-Q. Jiang and W.-X. Zhou, J. Phys. A **43**, 335002 (2010).
[124] S. Redner, Eur. Phys.J. B **4**, 131 (1998).
[125] F. Radicchi and C. Castellano, PloS One **7**, e33833 (2012).
[126] F. N. Silva, F. A. Rodrigues, O. N. de Oliveira Jr and L. da F. Costa, J. of Informetrics **7**, 469 (2003).